



LEEDS  
BECKETT  
UNIVERSITY

---

Citation:

Cassano, A and Marchese Robinson, RL and Palczewska, A and Puzyn, T and Gajewicz, A and Tran, L and Manganelli, S and Cronin, MTD (2016) Comparing the CORAL and Random Forest approaches for modelling the in vitro cytotoxicity of silica nanomaterials. *Alternatives to Laboratory Animals*, 44 (6). pp. 533-556. ISSN 0261-1929 DOI: <https://doi.org/10.1177/026119291604400603>

Link to Leeds Beckett Repository record:

<https://eprints.leedsbeckett.ac.uk/id/eprint/5729/>

Document Version:

Article (Accepted Version)

---

Creative Commons: Attribution-Noncommercial-No Derivative Works 4.0

The aim of the Leeds Beckett Repository is to provide open access to our research, as required by funder policies and permitted by publishers and copyright law.

The Leeds Beckett repository holds a wide range of publications, each of which has been checked for copyright and the relevant embargo period has been applied by the Research Services team.

We operate on a standard take-down policy. If you are the author or publisher of an output and you would like it removed from the repository, please [contact us](#) and we will investigate on a case-by-case basis.

Each thesis in the repository has been cleared where necessary by the author for third party copyright. If you would like a thesis to be removed from the repository or believe there is an issue with copyright, please contact us on [openaccess@leedsbeckett.ac.uk](mailto:openaccess@leedsbeckett.ac.uk) and we will investigate on a case-by-case basis.

1 **Comparing the CORAL and Random Forest approaches for modelling the *in vitro***  
2 **cytotoxicity of silica nanomaterials**

3 Antonio Cassano<sup>a</sup>, Richard L. Marchese Robinson<sup>a</sup>, Anna Palczewska<sup>b</sup>, Tomasz Puzyn<sup>c</sup>, Agnieszka Gajewicz<sup>c</sup>,  
4 Lang Tran<sup>d</sup>, Serena Manganelli<sup>e</sup>, Mark T. D. Cronin<sup>\*a</sup>

5 <sup>a</sup>*School of Pharmacy and Biomolecular Sciences, Liverpool John Moores University, Byrom Street, Liverpool, L3*  
6 *3AF, England.*

7 <sup>b</sup>*University of Leeds, School of Geography, Leeds, England.*

8 <sup>c</sup>*Laboratory of Environmental Chemistry, University of Gdansk, Wita Stwosza 63, 80-308 Gdansk, Poland.*

9 <sup>d</sup>*Institute of Occupational Medicine, Edinburgh, Midlothian, Scotland.*

10 <sup>e</sup>*IRCSS-Istituto di Ricerche Farmacologiche Mario Negri, Via Giuseppe La Masa, 19, 20156, Milan, Italy.*

11

12 **Summary**

13 Nanotechnology is one of the most important technological developments of the twenty-first century. In silico  
14 methods such as quantitative structure-activity relationships (QSARs) to predict toxicity promote the safe-by-  
15 design approach for the development of new materials, including nanomaterials. In this study, a set of cytotoxicity  
16 experimental data corresponding to 19 data points for silica nanomaterials was investigated to compare the widely  
17 employed CORAL and Random Forest approaches in terms of their usefulness for developing so-called “nano-  
18 QSAR” models. “External” leave-one-out cross-validation (LOO) analysis was performed to validate the two  
19 different approaches. An analysis of variable importance measures and signed feature contributions for both  
20 algorithms was undertaken in order to interpret the models developed. CORAL showed a more pronounced  
21 difference between the average coefficient of determination ( $R^2$ ) between training and LOO (0.83 and 0.65 for  
22 training and LOO respectively) compared to Random Forest (0.87 and 0.78 without bootstrap sampling, 0.90 and  
23 0.78 with bootstrap sampling), which may be due to overfitting. The aspect ratio and zeta potential from amongst  
24 the nanomaterials’ physico-chemical properties were found to be the two most important variables for the Random  
25 Forest and the average feature contributions calculated for the corresponding descriptors were consistent with the  
26 clear trends observed in the dataset: less negative zeta potential values and lower aspect ratio values were  
27 associated with higher cytotoxicity. In contrast, CORAL failed to capture these trends.

28

29 *Keywords:* pseudo-SMILES; nano-QSAR; CORAL software; Random Forest; silica nanoparticle; variable  
30 importance; feature contribution

31 <sup>\*</sup>Corresponding author at: School of Pharmacy and Biomolecular Sciences, Liverpool John Moores University,  
32 Byrom Street, Liverpool, L3 3AF, England. *Email address:* M.T.Cronin@ljmu.ac.uk

## 33 1. Introduction

34 Nanotechnology, which may be defined as the technological application of engineered nanomaterials [1],  
35 is considered to be one of the most important technological developments of the 21<sup>st</sup> century [2, 3] so  
36 much so that the term “nano-revolution” has been used to describe the growth of this industry [4].  
37 Nanotechnology is able to produce engineered nanomaterials having new or enhanced physico-chemical  
38 properties compared to the bulk material. However, some of these properties, e.g. high surface area to  
39 volume ratio, are potentially dangerous to humans [5-9]. *In silico* methods (e.g. (Q)SAR, grouping and  
40 read-across) promote the safe-by-design approach for the development of new nanomaterials by studying  
41 the relationship between the nanomaterials’ “structures” and their biological effects [10, 11]. Since  
42 nanomaterials are complex [12], typically polydisperse, particulate materials, the concept of a “structure”  
43 in this context should not be confused with a single molecular structure but rather a description of the  
44 nanomaterial in terms of its measurable physico-chemical characteristics [9, 13] such as the composition  
45 of different components, aspect ratio etc. In this regard, the development of nanomaterial quantitative  
46 structure-activity relationships (“nano-QSAR”) may offer an effective alternative to experimental testing,  
47 since they may enable the prediction of (eco)toxicological effects of nanomaterials based on a knowledge  
48 of their chemical composition and, where necessary, other physico-chemical properties [14-16]. QSAR  
49 models can be classified as linear or non-linear depending on whether they were developed using a linear  
50 method, such as a multiple linear regression [17, 18], or a non-linear methods, such as support vector  
51 machines in combination with a non-linear kernel function [19, 23] or Random Forest [24, 25]. The aim  
52 of this study was to evaluate different approaches to build nano-QSAR models for a dataset comprising  
53 19 cytotoxicity experimental data points for silica nanomaterials. We focused on silica nanomaterials  
54 mainly because of the availability of a novel experimental dataset for nanomaterials with a silica core and  
55 due to the widespread use of silica based nanomaterials in consumer products  
56 (<http://www.nanotechproject.org/cpi/browse/nanomaterials/silicon-dioxide/>). In this work, a comparison  
57 was made between two commonly used approaches to develop QSAR and nano-QSAR models: the linear  
58 approach implemented in the COrelation And Logic (CORAL) program, which optimises a (linear)  
59 regression model using a Monte Carlo search procedure [26], and Breiman’s non-linear Random Forest  
60 algorithm [24, 25], implemented in the R randomForest package [27]. Our motivation to focus on these  
61 two modelling approaches reflects the fact that these have been used to build QSAR/QSPRs (and nano-  
62 QSAR/QSPRs) for a variety of different datasets, as illustrated in the number of publications summarised  
63 in the Supplementary Information (SI); for instance, 28 and 21 articles describing QSAR/QSPRs and

64 nano-QSAR/QSPRs studies using the COARL and Random Forest approaches respectively, were  
65 published in 2015. (Quantitative structure-property relationships, or QSPRs, are analogous to QSARs,  
66 but aim to predict non-biological properties.) However, to the best of our knowledge, these algorithms  
67 have never previously been compared. Indeed, Random Forest has only twice before been used to model  
68 nanomaterial effects [28, 29]. Hence, this investigation serves as a timely comparison of two widely  
69 employed QSAR modelling approaches on a suitable dataset. In addition to comparing their predictive  
70 performance, we performed a comparison in terms of model interpretability between a linear (CORAL)  
71 and a non-linear (Random Forest) approach. In other words, the ability of the two selected approaches to  
72 describe the toxicological trends of this dataset was evaluated.

## 73 **2. Materials and Methods**

### 74 **2.1. Experimental data**

75 The experimental data used to develop the models correspond to a subset extracted from the dataset  
76 generated during the MODENA COST Initiative (MODENA TD1204 COST ACTION dataset,  
77 <http://www.modena-cost.eu/Home.aspx>). This dataset is provided in Table 1 and it is available  
78 electronically in the SI. The dataset consists of 19 *in vitro* WST-1 cytotoxicity experimental data points  
79 for uncoated silica nanomaterials. Briefly, WST-1 is a colorimetric assay for assessing cell metabolic  
80 activity which is similar to the MTT assay, but which offers certain experimental advantages [30, 31].  
81 The changes in metabolic activity measured using the WST-1 assay are considered a proxy for changes  
82 in cell viability [32]. The data used in this work consist of 19 values for the negative logarithm of the  
83 EC<sub>25</sub> i.e. the concentration level which induces 25% of maximum response above the baseline after a  
84 given treatment time. For modelling, nanomaterial concentrations, hence the corresponding EC<sub>25</sub> values,  
85 were expressed as surface area of nanomaterial per millilitre (i.e. mm<sup>2</sup>/ml), in keeping with guidance from  
86 the Organisation for Economic Co-operation and Development [33]. Cytotoxicity data range from -1.299  
87 to 0.483, with no values between -0.822 and -0.394 i.e. the data cluster at low and high activities as shown  
88 in Figure 1. Furthermore, from the original dataset we selected five variables based on our expert  
89 judgement expected to explain variability in these activities: treatment time and cell type are related to  
90 the experimental conditions adopted in the assay protocol, whereas average size, aspect ratio and zeta  
91 potential are measured physico-chemical properties of silica nanomaterials. Specifically, since CORAL  
92 is only able to handle a maximum of five variables, less significant descriptors were discarded. The full  
93 list of descriptors can be found in the SI.

## 94 2.2. Evaluation approach

95 We adopted an “external” leave-one-out (LOO) cross-validation technique as a method to validate the  
96 considered modelling approaches. In brief, LOO is a special case of cross-validation [34-36], where the  
97 number of folds equals the number of instances in the data set. In other words, the learning algorithm is  
98 applied once for each instance, using all other instances as a training set and using the selected instance  
99 as a single-item test set. To this respect, for the dataset used in this work which comprises 19 instances,  
100 both CORAL and Random Forest algorithms were applied 19 times over all the instances in the dataset,  
101 each time considering 18 instances as training set and the remaining one as a test set in order to generate  
102 a given set of LOO results. (For both methods, five sets of LOO results were obtained as explained below.)  
103 By “external” LOO, we mean that all model development – including selection of descriptors and  
104 algorithm parameters or “hyperparameters” – was carried out exclusively using each LOO training set in  
105 turn i.e. the biological activity of the correspond test instance was not considered, to remove this potential  
106 source of optimistic bias from the results [37-39]. The coefficient of determination ( $R^2$ ) and the root mean  
107 square error (RMSE) were here used as statistics for comparing the two approaches, according to the  
108 equations (1) and (2) [36], based on two n value vectors  $y_1...y_n$  and  $f_1...f_n$  which are associated with the  
109 experimental and predicted values respectively. N.B. (a) As the dataset comprised 19 instances,  $n = 18$   
110 for training sets whereas  $n = 19$  for LOO. (b) In equations (1) and (2), and all subsequent equations in this  
111 manuscript, the “ $\bar{\phantom{x}}$ ” character indicates the arithmetic mean (or “average”) value over all the elements of  
112 a vector.

113

$$114 \text{ Coefficient of determination} = R^2 = 1 - \frac{\sum_{i=1}^n (y_i - f_i)^2}{\sum_{i=1}^n (y_i - \bar{y})^2} \quad (1)$$

115

$$116 \text{ Root mean square error} = \text{RMSE} = \sqrt{\frac{\sum_{i=1}^n (y_i - f_i)^2}{n}} \quad (2)$$

117

118 We performed the LOO validation technique five times, since the CORAL and Random Forest algorithms  
119 employ random selections during the model building phase, in order to obtain a more robust estimate of  
120 the performance of these methods. We selected five different seeds for each repetition with the Random  
121 Forest algorithm. We further selected five different dataset partitions for each repetition with CORAL.  
122 (Each time the CORAL software is run, it automatically generates a random seed that cannot be set by

123 the end user.) Each dataset partition corresponds to partitioning of a given LOO training set, following  
124 removal of a single test set instance for “external” LOO validation, to yield an internal “test set” for  
125 hyperparameter selection. Repeating modelling with CORAL five times in this fashion is broadly in  
126 keeping with the recommended procedure for CORAL model optimisation and robustness evaluation [40-  
127 42]. Further discussion of the CORAL hyperparameters which were optimised is presented under  
128 “CORAL modelling”. The average ( $\bar{a}$ ), standard deviation ( $s$ ) and standard error of the mean (SE) for the  
129 LOO  $R^2$  and RMSE statistics across the five different repetitions were calculated as shown in equations  
130 (3), (4) and (5), considering the three general formulas based on a vector of  $m$  values i.e.  $a_1, a_2, \dots, a_m$ .  
131 N.B. Here,  $m = 19$  for training set results averaged for a single seed (or CORAL training set split), or 95  
132 ( $19 \times 5$ ) for “global” training set results, whereas  $m = 5$  for LOO results.

133

134 **Average** =  $\bar{a} = \frac{1}{m} \sum_{i=1}^m a_i$  (3)

135

136 **Standard deviation** =  $s = \sqrt{\frac{\sum(a_i - \bar{a})^2}{(m-1)}}$  (4)

137

138 **Standard error of the mean** =  $SE = \frac{s}{\sqrt{m}}$  (5)

139

### 140 **2.3. Descriptor calculations**

141 As is further explained under “CORAL modelling”, continuous numeric properties, such as zeta potential,  
142 were converted into binary descriptors corresponding to labels applied to specific ranges: each descriptor  
143 took a value of 1 (or 0) if the corresponding property value for a given instance was inside (or outside) of  
144 this range. In the case of the discrete qualitative variable “Cell Type”, each value was converted into a  
145 binary descriptor: the descriptor took the value 1 (or 0) if the “Cell Type” for a given instance matched  
146 (or did not match) the value associated with that descriptor. This was necessary since, as is explained  
147 under “CORAL modelling”, the CORAL algorithm can only work with binary descriptors. These binary  
148 descriptors were used for both CORAL and Random Forest modelling. For the CORAL software, these  
149 descriptors were represented implicitly i.e. the presence of a corresponding label in a pseudo-SMILES  
150 (see “CORAL modelling”) denotes a descriptor value of 1. For the implementation of Random Forest

151 used in the current work (see “Random Forest modelling”), these binary descriptors were represented as  
152 an explicit bit-string.

#### 153 **2.4. Correlated descriptors**

154 We tested the influence of correlated descriptors on model results for both CORAL and Random Forest  
155 approaches by generating two versions of the original dataset, as shown in Table 2. In one case, after the  
156 binary splitting was applied to each continuous numeric variable, a label was assigned to each of the  
157 generated value ranges, which translates into two perfectly correlated descriptors for a given continuous  
158 numeric variable. For instance, by splitting the “Treatment Time” variable into 24 and 48 hours, we  
159 generated two labels, namely “A” and “B”, which refer to the 24 and 48 hours’ exposure respectively, in  
160 the *in vitro* model. This results in the generation of two perfectly correlated descriptors, since they are  
161 mutually exclusive. Specifically, when the “A” label is applicable (i.e. the “A” descriptor value is 1), the  
162 “B” label must not be applicable (i.e. the “B” descriptor value is 0), and vice-versa, according to the fact  
163 that, a single experimental result can only be associated with a single “Treatment Time” value. In the  
164 second case, after the splitting of the continuous numeric variables, only one of the ranges was assigned  
165 a label and, hence, a corresponding binary descriptor. As a result, perfectly correlated descriptors were  
166 removed. For the sake of brevity, even though the second approach does use correlated descriptors for the  
167 cell line variable, throughout this paper results obtained “with correlated descriptors” refer to the first  
168 approach i.e. two labels for each continuous numeric variable, whereas results obtained “without  
169 correlated descriptors” refer to the second approach. In the main text of this paper, only results obtained  
170 without correlated descriptors were presented, with results obtained with correlated descriptors presented  
171 in the SI for comparison.

172

#### 173 **2.5. CORAL modelling**

174 In this work, the Monte Carlo algorithm implemented in the CORAL software (version: December 17,  
175 2014 for Microsoft Windows, available at <http://www.insilico.eu/coral/>) was used as a tool for developing  
176 linear nano-QSAR models, taking into account both the information derived from the nanomaterials’  
177 physico-chemical properties (e.g. zeta potential) and the experimental conditions (e.g. cell type).  
178 Specifically, after we downloaded the zipped file from the aforementioned website containing the binary  
179 executable files, we executed the CORAL.exe binary file included in the folder  
180 “CORALSEA\MyCORALSEA\REGRESSION” to perform the modelling. In keeping with earlier work,  
181 we generated a “pseudo-SMILES” string for each instance which represented both information related to

182 particular experimental conditions and nanomaterial properties [40]. In more detail, with this particular  
183 approach, all the eclectic information is used for modelling, with the endpoint of interest being a function  
184 of both the nanomaterials' physico-chemical properties and experimental conditions. Pseudo-SMILES  
185 character strings were derived as shown in Table 2. When used to build linear models, as in the current  
186 work, the CORAL algorithm effectively treats each character (or label) in the pseudo-SMILES strings as  
187 a binary descriptor which takes a value of 1 (or 0) if the character is present (or absent) for a given instance  
188 [40, 43]. The manner in which predictions are obtained, based on the values of these descriptors for a  
189 given instance, is further explained when discussing "Variable importance" below (see equations 6 and  
190 7). Table 2 shows the selected labelling approaches with and without correlated descriptors, but we  
191 reported in the main text only results obtained without correlated descriptors (leave-one-out results  
192 obtained with correlated descriptors can be found in the SI). For the current dataset, after removing  
193 correlated descriptors, pseudo-SMILES labels were generated as follows. The information on the cell  
194 type was coded with the 'C', 'D', 'E', 'F' and 'G' characters for the 16HBE, A549, HaCaT, NRK-52E  
195 and THP-1 cell types, respectively. For all numeric descriptors in the dataset, a "binary split" was  
196 performed i.e. numeric values beyond some threshold were assigned a label and values before that  
197 threshold were not, thus avoiding incorporating perfectly correlated descriptors. Specifically, for the  
198 treatment time descriptor, a label 'A' was assigned if the exposure time was 24 hours, whereas no label  
199 was assigned if the exposure time was 48 hours. For each of the three properties related to the  
200 nanomaterial physico-chemical properties, namely average size, aspect ratio and zeta potential, a binary  
201 split of the values was applied based on the median value for the dataset, with the rationale of having a  
202 similar number of instances in a given range for each property. (N.B. The odd number of instances – i.e.  
203 19 – in the dataset meant that the number of instances in each range, for each binary split, could not be  
204 perfectly equal and the ranges are expressed in terms of the values just beyond the median for aspect ratio  
205 and zeta potential.) The thresholds used for the splits were 27.5 (no label for values below or equal to the  
206 threshold, 'I' for values above it), 1.0 (no label for values equal to the threshold, 'K' for values above it)  
207 and -32.0 (no label for values below the threshold, 'L' for values equal to or greater than it) for the average  
208 size, aspect ratio and zeta potential, respectively. In earlier work with CORAL [40-42], the authors  
209 developed five different splits of the same dataset in order to check whether the developed models were  
210 obtained by chance. According to the recommended CORAL optimisation strategy, we selected the best  
211 hyperparameter values (i.e. N = number of epochs, T = threshold) using the model performance on a



212 subset of the dataset, which is called a “test set” in the CORAL software documentation, and then we  
213 predicted the single item “external” test set in a separate step after the model was built. For each LOO  
214 training set, modelling was repeated five times, via splitting the training set to yield an internal “test set”  
215 for hyperparameter selection, five times. More details on the application of the CORAL software to this  
216 dataset are reported in the SI, including full details of the five different LOO training set partitions used  
217 for hyperparameter selections. (See “Details on the CORAL software settings and optimisation” in the  
218 SI.)

219

## 220 **2.6. Random Forest modelling**

221 Random Forest is an ensemble learning method for both classification and regression which operates by  
222 building a multitude of decision trees, providing as output the class which represents the majority  
223 prediction, for classification problems, or the average prediction, for regression problems, of the  
224 individual trees [24, 25]. Each decision tree is grown using an independent random sample of the instances  
225 in the training set, with the descriptors considered for splitting each node being independently sampled  
226 from the total. In the current work, both bootstrap sampling of the training set, i.e. sampling of N from N  
227 with replacement, and sampling without replacement were considered. The results presented in the main  
228 text were obtained without bootstrap sampling, with results obtained with bootstrap sampling being  
229 reported in SI. Whilst bootstrap sampling is typically used [25, 27] it is not currently possible to calculate  
230 feature contributions (see the “Feature contribution analysis” section) with the available software [44] if  
231 bootstrap sampling is used. The results in the SI show that, for this dataset, the model performance and  
232 standard variable importance measures (see the “Variable importance” section) are very similar with both  
233 types of sampling. In this work, we used the Random Forest algorithm implemented in the randomForest  
234 R package (version 4.6-12) [27], with the default values for the algorithm “hyperparameters” i.e. number  
235 of trees to grow (ntree) equal to 500 and the number of descriptors randomly sampled at each split (mtry)  
236 equal to the total number of descriptors in the dataset divided by three (for regression problems) as  
237 explained in the randomForest package documentation. The experimental data used for Random Forest  
238 modelling were the same as for the CORAL software. The binary descriptors implicitly encoded in the  
239 pseudo-SMILES strings created for the CORAL software were explicitly represented for modelling using  
240 the randomForest package i.e. a “1” value was assigned each time a specific label was present whereas a  
241 “0” value was assigned each time the label was absent in the considered pseudo-SMILES. Using this  
242 procedure, an explicit bit string was built for each pseudo-SMILES, as shown in Table 3. As per modelling

243 with CORAL, with the Random Forest algorithm 95 models were developed with a given sampling  
244 protocol i.e. 19 models for each LOO training set and all modelling on a given training set was repeated  
245 five times to take account of the random sampling inherent to building models with Random Forest or  
246 CORAL. This process was repeated twice with two different sampling protocols: with simple sampling,  
247 without replacement, or bootstrap sampling i.e. the replace argument of the randomForest() function was  
248 set to FALSE and TRUE respectively. Hence, 190 Random Forest models were built in total with or  
249 without correlated descriptors. (It should be reiterated that only results “without correlated descriptors”,  
250 meaning without perfectly correlated descriptors, without bootstrap sampling are presented in the main  
251 text.)

252

## 253 **2.7. Variable importance**

### 254 **2.7.1. CORAL**

255 In the current work, we selected the additive scheme of the CORAL software which computes a so-called  
256 “optimal descriptor” (DCW) as the sum of correlation weights associated with the labels present in the  
257 pseudo-SMILES strings [40, 43], according to equation (6).

$$258 \text{DCW}(\text{Threshold}, N_{\text{epoch}})_i = \sum_{k=1}^5 \text{Cw}_k \times \text{SA}_{k,i} \quad (6)$$

259 N.B. In equation (6),  $\text{SA}_{k,i}$  takes the value 1 (or 0) if the corresponding pseudo-SMILES label is present  
260 (or absent) in an instance (i) i.e. the correlation weights ( $\text{Cw}_k$ ) are summed over all labels present in a  
261 given instance. In order to understand the relationship between the correlation weights and the final  
262 predicted value, it is important to note that the so-called “optimal descriptor” is used to calculate the  
263 predicted value for the endpoint using a one variable linear equation, as shown in equation (7).

$$264 \text{Prediction}_i = \text{C}_0 + \text{C}_1 * \text{DCW}(\text{Threshold}, N_{\text{epoch}})_i \quad (7)$$

265 Hence, it can be seen that the correlation weights are essentially scaled values of (i.e. are directly  
266 proportional to) the coefficients of the binary descriptors in the final linear model developed using  
267 CORAL. In order to make a comparison between CORAL and the standard Random Forest methods for  
268 variable importance, we calculated the absolute values of the correlation weights for each descriptor. This  
269 is because the Random Forest standard variable importance measures do not take account of the sign of  
270 the contribution a given descriptor value makes towards the prediction.

271

272

### 273 2.7.2. Random Forest

274 The Random Forest algorithm implemented in the randomForest R package which was used in this work  
275 provided information on variable importance using two approaches, by setting the “importance” option  
276 of the randomForest function to TRUE. The first method [25] calculates the percentage increase of the  
277 mean squared error (“%IncMSE”) on the out-of-bag (OOB) subset – i.e. the subset of training set  
278 instances not used to build a given tree - after the permutation of descriptors’ values. In greater detail, for  
279 each tree in the forest, the prediction error on the OOB portion of the data, expressed by the mean square  
280 error (MSE) is recorded (for regression problems). The MSE value is then calculated again after  
281 permuting each predictor variable one at a time. The differences between the two calculated MSEs for  
282 the original and shuffled datasets are averaged over all trees and then normalised by the standard deviation  
283 of the differences. The second method (“IncNodePurity”) calculates the total decrease in node  
284 “impurities” from splitting on a given descriptor, averaged over all the generated trees. For regression,  
285 “impurity” is measured by the residual sum of squares (RSS) metric for a given node [27].

286

### 287 2.8. Summarising Variable Importance Values

288 The different variable importance approaches employed with Random Forest and CORAL are applicable  
289 for a single model, hence – in order to derive general conclusions – it was necessary to summarise these,  
290 for a given combination of modelling approach and variable importance approach, over all 95 (19 LOO  
291 training sets  $\times$  5 repetitions) models. Furthermore, it was necessary to take account of the fact that the  
292 different approaches could vary in scale – which would confound comparisons. Hence, the raw values ( $v$ )  
293 – for a given combination of modelling approach and variable importance approach – were scaled ( $v_{\text{scaled}}$ )  
294 between 0 and 1 as per equation (8), where the minimum ( $v_{\text{min}}$ ) and maximum ( $v_{\text{max}}$ ) values were obtained  
295 across all 95 models and all 5 descriptors. Subsequently, the values were summarised in terms of the  
296 arithmetic mean and the corresponding standard error of the mean.

297

$$298 \quad v_{\text{scaled}} = \frac{(v - v_{\text{min}})}{(v_{\text{max}} - v_{\text{min}})} \quad (8)$$

299

### 300 2.9. Feature contribution analysis

301 By “feature contribution analysis”, we refer to estimates of both the sign and magnitude of the influence  
302 a given descriptor has on the prediction made by a given model, in contrast to “variable importance”

303 measures which only estimate the magnitude of the influence. As far as the CORAL software is  
304 concerned, we calculated feature contributions based on the signed values of the correlation weights.  
305 Indeed, as equations (6) and (7) show (see the “Variable importance” section), for each single model  
306 which is obtained by selecting the additive method, the signed values of the correlation weights allow  
307 understanding of whether a certain descriptor is contributing “positively”, i.e. it contributes to increased  
308 toxicity, or “negatively”, i.e. it contributes to decreased toxicity. For Random Forest, a feature  
309 contribution analysis was carried out using the technique developed by Kuz'min and colleagues [45] and  
310 implemented in the rFC R package [44] which is designed to work with the randomForest  
311 implementation of Random Forest. (Specifically, version 1.0 of rFC, as obtained via the  
312 “install.packages("rFC",repos="http://R-Forge.R-project.org)”) command, was used in the current  
313 work). This feature contribution method is a measure of the influence, in terms of the magnitude and sign,  
314 of each variable on the model prediction for a single instance. In principle, the feature contribution  
315 associated with the value of a given descriptor could vary between instances with the same value for that  
316 given descriptor, due to the fact that Random Forest models are non-linear. In contrast, the feature  
317 contribution associated with a single descriptor as calculated for CORAL is either equal to the value of  
318 the corresponding correlation weight (if the descriptor value is 1) or 0 (if the descriptor value is 0). Hence,  
319 to enable a comparison between the average influence of a given descriptor value being 1 for both CORAL  
320 and Random Forest, pseudo-coefficients were derived from the Random Forest feature contributions.  
321 These pseudo-coefficients were calculated by computing, for each descriptor, the difference between the  
322 arithmetic mean average values calculated over the feature contribution values for the pseudo-SMILES  
323 strings having a value of 1 for that specific descriptor (here called FC(1)) and pseudo-SMILES strings  
324 having a value of 0 for the same descriptor (here called FC(0)), according to the equation (9).

325

$$326 \quad \text{Pseudo - coefficient} = \overline{\text{FC}(1)} - \overline{\text{FC}(0)} \quad (9)$$

### 327 3. Results

#### 328 3.1. LOO results

329 LOO results, in terms of  $R^2$  and RMSE for both CORAL and Random Forest algorithms are reported in  
330 Table 4. As far as the global results on the corresponding training sets are concerned, the average and  
331 standard error of the mean, over the 95 developed models, of the  $R^2$  and RMSE statistics were calculated  
332 for both CORAL and Random Forest models. N.B. In contrast to the results shown in Table 4, results

333 with perfectly correlated descriptors (for both CORAL and Random Forest) and bootstrap sampling (for  
334 Random Forest) are presented in the SI. Considering the LOO results reported in Table 4, it is clear that  
335 CORAL's LOO test set performance was substantially worse than its performance on the corresponding  
336 training sets. With respect to CORAL, the global average value of the  $R^2$  on training sets was 0.8285  
337 whereas the average RMSE was 0.2347. Results from LOO (i.e. testing) for CORAL showed a decrease  
338 for the average  $R^2$  to 0.6486, whereas the average value of the RMSE increased to 0.3456. However, the  
339 corresponding results for Random Forest showed a smaller reduction in estimated model performance  
340 upon going between training and LOO test global results. The average values of  $R^2$  were 0.8723 and  
341 0.7807 for training and test set respectively and the average values for RMSE were 0.2011 and 0.2604  
342 for training and test set respectively. If one considers only results from the LOO test sets in Table 4, it  
343 can be stated that Random Forest performed better than CORAL and the smaller reduction in average  
344 model performance upon going from the training to the test sets indicates Random Forest did not overfit  
345 as much. As far as single run results are concerned, as shown in Table 4 for CORAL software, the average  
346  $R^2$  values on LOO training sets, for different splits of the same LOO training sets to yield internal "test  
347 sets" for hyperparameter selection, ranged between 0.7876 and 0.8570. (Here, it should be remembered  
348 that – for a given split of the data to yield internal "tests sets" for each LOO training set – the results were  
349 averaged across all 19 LOO training sets.) Corresponding LOO  $R^2$  test set values ranged between 0.6143  
350 and 0.7082. Average RMSE values for different splits of the CORAL input dataset ranged from 0.2119  
351 and 0.2675 on training sets whereas RMSE values on test sets ranged between 0.3010 and 0.3712. The  
352 Random Forest approach showed less variability, in terms of both  $R^2$  and RMSE, among the five runs of  
353 the software with different seeds. Indeed, average training set  $R^2$  values ranged between 0.8711 and  
354 0.8736, whereas LOO test set  $R^2$  values ranged between 0.7707 and 0.7899. Moreover, according to Table  
355 4, Random Forest average RMSE values ranged between 0.1995 and 0.2022 on training sets whereas on  
356 LOO test sets RMSE values ranged between 0.2544 and 0.2665. It is important to note that, among the  
357 five runs of LOO for the CORAL software, the largest difference in the  $R^2$  values between training and  
358 test sets is 0.2427 (split 3) whereas, for Random Forest, the largest difference is 0.1004. Taking into  
359 account the reference value for the difference of  $R^2$  between training and test sets reported in the article  
360 of Eriksson and colleagues [46], the average results obtained with CORAL are closer than Random Forest  
361 to the 0.3 threshold for which a model could be considered to overfit. Additional results obtained with  
362 CORAL and Random Forest under different scenarios are presented in Table S1 in the SI. Firstly, it can

363 be observed that no significant training/test set performance gap exists for Random Forest if the training  
364 set is predicted using only out-of-bag samples. Furthermore, the comparison of the results obtained with  
365 and without correlated descriptors for the dataset used in this work showed that Random Forest is, as  
366 expected [25], less affected than CORAL by the presence of correlated descriptors (see Table S1 in SI).  
367 Specifically, the split number 2 of the CORAL input dataset generated an outlier only when perfectly  
368 correlated descriptors were used. For Random Forest, a very small difference in terms of  $R^2$  and RMSE  
369 global average values was observed for results with and without bootstrap sampling.

370

### 371 **3.2. Variable importance results**

372 Figure 2 shows the average and standard error of the mean (as error bars) of the scaled variable importance  
373 values for each descriptor and each variable importance measure for CORAL and Random Forest. N.B.  
374 In contrast to the results shown in Figure 2, results with perfectly correlated descriptors (for both CORAL  
375 and Random Forest) and bootstrap sampling (for Random Forest) are presented in the SI (Figures S1 and  
376 S2). As far as CORAL is concerned, the average values ranged between 0.0525 and 0.8941 for the K and  
377 L descriptors, respectively, which are related to the nanoparticle aspect ratio (i.e. aspect ratio  $> 1$ ) and  
378 zeta potential (zeta potential  $\geq -32.0$  mV) nanomaterial physico-chemical properties respectively. Hence,  
379 according to the CORAL variable importance measure, the nanoparticle aspect ratio and zeta potential  
380 were respectively the least and most important variables related to cytotoxicity. With respect to the  
381 Random Forest %IncMSE method, the average values ranged between 0.0424 and 0.8393 for the G and  
382 L descriptors which are related to the THP-1 cell line and zeta potential respectively. On the other hand,  
383 Random Forest IncNodePurity method average values ranged between 0.0124 and 0.8181 for the E and  
384 L descriptors which refer to the HaCaT cell line and zeta potential respectively. In spite of small  
385 differences depending upon the specific method used, the descriptors (K and L) corresponding to aspect  
386 ratio and zeta potential are (on average) by far the most important according to both the Random Forest  
387 variable importance measures. Conversely, even if CORAL also identified the descriptor corresponding  
388 to zeta potential as the most important, descriptors D and G corresponding to cell lines A549 and THP-1,  
389 respectively are the second and third most important variables. Furthermore, Random Forest variable  
390 importance results with perfectly correlated descriptors also support the conclusion that aspect ratio and  
391 zeta potential are the most toxicologically relevant variables, confirming that the Random Forest approach  
392 is not significantly affected by correlated descriptors (see Figure S2 in SI). Similarly, Random Forest

393 variable importance results obtained without bootstrap sampling were largely consistent with those  
394 obtained with bootstrap sampling, for both %IncMSE and IncNodePurity methods (see Figure S1 and  
395 Figure S2 in SI). CORAL variable importance results with correlated descriptors showed that the two  
396 most important variables were the J and L descriptors, corresponding to the aspect ratio and zeta potential.  
397 However, it is important to note that, unlike for Random Forest, the other descriptors corresponding to  
398 aspect ratio and zeta potential are not similarly important. It is also important to note that, for CORAL,  
399 the variable importance values calculated with or without perfectly correlated descriptors were not as  
400 consistent as compared to Random Forest.

### 401 **3.3. Feature contribution results**

402 Figure 3 shows the average values, for both CORAL correlation weights and Random Forest feature  
403 contribution pseudo-coefficients, calculated across all the 95 models generated on the LOO training sets,  
404 without perfectly correlated descriptors and without bootstrap sampling for Random Forest. (Results with  
405 perfectly correlated descriptors are presented in SI Figure S3.) Broadly in keeping with what was observed  
406 for the variable importance analysis (Figure 2), for Random Forest aspect ratio and zeta potential  
407 nanoparticles' physico-chemical properties were the two most important variables whereas, for the  
408 CORAL approach, zeta potential and the variable related to the A549 cell line appear most important.  
409 Hence, as expected, feature contribution results are consistent with those obtained for variable importance  
410 for both approaches. It is important to note that, for CORAL approach, feature contribution average values  
411 were all positive. Conversely, Random Forest feature contribution results presented both positive and  
412 negative values. Specifically, for the CORAL approach, the correlation weight associated with the zeta  
413 potential feature had a magnitude that is more than double of the A549 cell line magnitude; whereas for  
414 Random Forest the two highest feature contribution values have a similar magnitude. In addition, in  
415 contrast to CORAL, for Random Forest there is a considerable difference between the average influence  
416 of the two most important descriptors (relating to aspect ratio and zeta potential) and the others. These  
417 observations regarding the importance of different variables according to the feature contributions  
418 calculations (Figure 3) are broadly in keeping with those observed when perfectly correlated descriptors  
419 are not excluded (Figure S3). Results with correlated descriptors in the SI (Figure S3) showed that once  
420 again for Random Forest approach zeta potential and aspect ratio were the two most important properties.  
421 Specifically, considering the two correlated descriptors for aspect ratio and zeta potential, namely the J  
422 and K labels for aspect ratio and the L and M labels for zeta potential, it is worth noting that, for Random

423 Forest, the magnitudes of their average feature contribution values were not only very similar (roughly  
424 0.23) but also much greater than the magnitudes for the other descriptors. Conversely, for CORAL, we  
425 obtained average feature contributions of significantly different magnitude for the two correlated  
426 descriptors related to the same variable, both for aspect ratio and zeta potential properties. When the  
427 signed values are considered (Figure 3 or Figure S3), it is worth noting that for Random Forest high values  
428 of zeta potential are associated with an increase in cytotoxicity, whereas high aspect ratio values are  
429 associated with a decrease of toxicity since the average pseudo-coefficient value is negative for the  
430 corresponding descriptors. It is important to note that these findings are consistent with the preliminary  
431 analysis of the dataset reported in Figure 1. Conversely, the CORAL approach seems to only be able to  
432 partially recognise the trend in the data for the zeta potential. The descriptor associated with higher zeta  
433 potential values has a positive average feature contribution value, regardless of whether perfectly  
434 correlated descriptors were removed (Figure 3) or not (Figure S3). However, when perfectly correlated  
435 descriptors are not removed, the average feature contribution value for the descriptor corresponding to  
436 lower zeta potential values is still positive, even if less so (Figure S3). Whether perfectly correlated  
437 descriptors were removed (Figure 3) or not (Figure S3), the average feature contribution value for both  
438 descriptors corresponding to aspect ratio was positive.

#### 439 **4. Discussion**

440 Taking into account the results obtained in this comparison work, both in terms of their predictive  
441 performance estimated via “external” LOO validation and their ability to be interpreted to reveal trends  
442 in the data, the non-linear Random Forest approach performed better than the linear CORAL approach  
443 for the specific dataset used in this paper. With respect to Random Forest, the difference for both  $R^2$  and  
444 RMSE average values between training and test sets was smaller and it had better results on the test set  
445 compared to CORAL (Table 4). In addition, for Random Forest both average  $R^2$  and RMSE values for  
446 the OOB and LOO predictions methods were very similar, regardless of whether modelling was  
447 performed with or without bootstrap sampling and with or without correlated descriptors (Table S1). This  
448 is interesting since it suggests that, even for these small datasets, as is typical for nano-QSAR studies [47],  
449 there may be no need to cross-validate Random Forest models as opposed to simply reporting their OOB  
450 performance. (Of course, for comparing to other methods, cross-validation would still be required for a  
451 fair, like-for-like comparison). However, it must be noted that this finding may not hold in general, e.g.  
452 Ballester and Mitchell found the OOB predictions only converged to the test set performance as the



453 training set got larger [48]. Currently, there is an on-going discussion on the importance of so-called  
454 intrinsic and extrinsic properties as well as composition of nanoparticles for toxicological studies [10, 13,  
455 49]. In our work, we incorporated various intrinsic (e.g. average primary particle size) and extrinsic (e.g.  
456 zeta potential) properties as descriptors for the modelled toxicity endpoint. We further sought to take  
457 account of variability in the endpoint values due to the different experimental conditions, by treating the  
458 varied experimental conditions as additional descriptors, as per the so-called “eclectic” approach  
459 previously proposed in the literature [41, 42, 50]. The variable importance analysis performed in this work  
460 showed that the aspect ratio and zeta potential nanoparticles’ physico-chemical properties were the most  
461 important variables for the Random Forest approach under all modelling scenarios with or without  
462 perfectly correlated descriptors and with or without bootstrap sampling (Figure 2, Figure S1 and Figure  
463 S2). This was not observed for CORAL. For example, when modelling was carried out without perfectly  
464 correlate descriptors (Figure 2), the two most important descriptors related to zeta potential and the A549  
465 cell line. In contrast to the results obtained with Random Forest, for which the most important descriptors  
466 - associated with zeta potential and aspect ratio - were comparably important, zeta potential was more  
467 important for CORAL than the A549 cell line, which had a comparable importance to the THP-1 cell line  
468 (Figure 2). However, it must be noted that descriptors related to cell line appear relatively less important  
469 when perfectly correlate descriptors are not removed from CORAL modelling (Figure S2). Regarding the  
470 observations concerning the importance of descriptors related to cell lines, Kim and colleagues [51]  
471 recently reported that cell type more than other factors like nanoparticles’ size and dose level can influence  
472 cytotoxicity and, in addition, in the same work they stated that identical nanoparticles’ preparations yield  
473 different outcomes depending on the selected cell lines even if they belong to the same cell type. Whilst  
474 our findings are not directly comparable, they still suggest that cell line is at least as important an  
475 experimental variable as average size, with the exact significance varying depending upon the specific  
476 cell line, the specific variable importance approach and modelling scenario (Figure 2, Figure S1 and  
477 Figure S2). As far as nanoparticles’ size is concerned, the work of Rong and colleagues [52] showed a  
478 potential important role of silica particles’ sizes in increasing toxicity towards endothelial cells. In another  
479 more relevant study, Tokgun and colleagues [53] reported results which showed that cytotoxicity towards  
480 A549 cell line depends on silica nanoparticles’ size. We found that the average size of silica nanoparticles  
481 was not typically (Figure 2, Figure S1 and Figure S2) amongst the most important variables but it did  
482 appear more significant when CORAL modelling was carried out including perfectly correlated

483 descriptors (Figure S2). Consider the clear trend observed in the dataset concerning the relationship  
484 between cytotoxicity and both zeta potential and aspect ratio (Figure 1) which was also reflected in the  
485 Random Forest variable importance (Figure 2, Figure S1 and Figure S2) and feature contributions (Figure  
486 3 and Figure S3) calculations. The clear correspondence between both the average Random Forest  
487 variable importance and feature contributions and the clear trends observed in the dataset makes it clear  
488 that our findings are not a result of an artefact of modelling but rather a consequence of the experimental  
489 dataset used in this work. However, these clear trends observed in the dataset appear to be at odds with  
490 the literature. Various publications have previously considered the relationship between aspect ratio and  
491 zeta potential nanoparticles' physico-chemical properties and cytotoxicity. Regarding the toxicological  
492 significance of particle shape (as quantified via the aspect ratio), studies for both carbon nanotubes and  
493 silica nanoparticles (as per the current work) either reported that aspect ratio had no relationship to toxicity  
494 or that high aspect ratio particles are more toxic [54, 55]. In contrast, if we look at the specific dataset  
495 used in this work, as shown in Figure 1, high aspect ratio silica nanoparticles are clustered at the low  
496 toxicity side of the graph. This finding is also reflected in the average Random Forest pseudo-coefficients  
497 presented in Figure 3. This discrepancy may be due to several reasons, such as differences in other  
498 characteristics of nanomaterials or in the cytotoxicity protocol used or in the cell line adopted as well as  
499 the concentrations selected for the test. To this respect, the review of Fruijtier-Pöllöth and colleagues [56]  
500 has shown that it is difficult to compare studies that are based on different experimental conditions and  
501 nanomaterials since they could yield contradictory results, which might be due to diverse toxicological  
502 mechanisms involved. As far as the relationship between zeta potential and toxicity is concerned, Cho et  
503 al. [57] found that, for a set of metal/metal oxide/silica nanoparticles high positive zeta potential resulted  
504 in more cytotoxicity and Karunakaran et al. [58] also suggested that cytotoxicity of alumina and silica  
505 particles, both micro-sized and nanoparticles, increases as a result of positive zeta potential. In the current  
506 work, both the feature contribution analysis results, as shown in Figure 3, and the preliminary analysis of  
507 the data shown in Figure 1, revealed that less negative zeta potential values were associated with higher  
508 cytotoxicity and that this trend was clearly captured by Random Forest and, to a lesser extent, CORAL  
509 (see Figure 3 and Figure S3). Whilst this might be considered consistent with earlier indications that  
510 increasing zeta potential leads to higher cytotoxicity [57, 58], it must be stressed that these earlier studies  
511 indicated that it was specifically positive zeta potential values that led to higher cytotoxicity and all zeta  
512 potential values reported in the dataset used for the current work were negative. One possible confounding

513 factor here could be that zeta potential is highly dependent upon the composition of the medium in which  
514 it was measured [57] and the experimentalists who provided the data modelled in the current work  
515 indicated that zeta potential values were measured in water rather than the exposure medium used for  
516 cytotoxicity testing. Hence, the actual zeta potential values of the nanoparticles when they were exposed  
517 to the cells could differ from those reported in our dataset. Arguably, better mechanistic insight would be  
518 obtained if zeta potential values had been measured under biologically relevant conditions [49, 57]. It is  
519 also the case that future studies might build upon our work via incorporating additional descriptors into  
520 the models. Firstly, as shown in the electronic version of the dataset used in this work in the SI the original  
521 dataset from which this was derived included other nanomaterial characteristics and experimental  
522 variables that were not considered as descriptors in our current work e.g. serum concentration or  
523 dispersion protocol. Indeed, prior to modelling analyses, we selected only five variables to model,  
524 according to our expert judgement since serum concentration and, supposing stirring and vortexing  
525 protocols were comparable, dispersion protocol experimental values, for this specific dataset, were the  
526 same for 17 out of 19 instances of the original dataset. (The assumption that the stirring and vortexing  
527 protocols were comparable was based on guidance from the MODENA COST team responsible for this  
528 dataset.) Secondly, none of the parameters provided in the original dataset may be considered to capture  
529 the surface reactivity or dissolution of the studied silica nanoparticles. One way of partially addressing  
530 this in future work, other than making additional experimental measurements [13], would be to perform  
531 additional quantum-mechanical calculations to obtain new different descriptors, i.e. independent variables  
532 reflecting structural and chemical properties of the nanoparticles [14, 59]. Such variables could further  
533 enhance our understanding of the possible mechanism of toxicity of the studied nanoparticles.

## 534 **5. Conclusions**

535 In this work a comparison between the CORAL and Random Forest methods in predicting silica  
536 nanoparticles' cytotoxicity, based upon physico-chemical characteristics and experimental conditions  
537 encoded into pseudo-SMILES strings, was performed. It was demonstrated that the pseudo-SMILES  
538 encoding proposed for CORAL could be translated into descriptors which can be used with other  
539 modelling approaches, such as Random Forest. LOO was used to externally validate the results obtained  
540 from the modelling task. The predictive performance estimated from LOO was significantly higher with  
541 Random Forest and substantially less overfitting was observed. Different approaches were employed to

542 analyse the significance of different descriptors within both kinds of models, including the derivation of  
543 pseudo-coefficients for Random Forest models that, in contrast to standard variable importance measures,  
544 reflect the signed contribution of descriptors towards the modelled endpoint. Whilst differences were  
545 observed with the different approaches to interpreting the models, the Random Forest approach, more  
546 than CORAL, reflected the toxicological significance of zeta potential and aspect ratio observed from  
547 preliminary analysis of the dataset. Interestingly, whilst these properties have previously been reported as  
548 significant for nanomaterial toxic effects, the relationships observed here were not in complete agreement  
549 with some previous studies – which could reflect different mechanisms. In summary, the results obtained  
550 suggest the Random Forest modelling approach is readily applicable to modelling the cytotoxicity of  
551 nanoparticles and can be used to develop models which offer reasonable predictive power and which can  
552 be interpreted in terms of physico-chemical-toxicity relationships.

### 553 **Acknowledgements**

554 MC and RLMR are grateful for funding from the European Union Seventh Framework Programme  
555 (FP7/2007-2013) under grant agreement number 309837 (NanoPUZZLES project). TP and AG are  
556 grateful for funding from the Polish Ministry of Science and Higher Education under grant agreement DS  
557 530-8637-D510-15. The MODENA COST Initiative (Grant Information - COST TD1204 'MODENA')  
558 and its experimental partners are thanked for providing the experimental data used in this work. The  
559 authors also thank Dr. Andrey A. Toropov and Dr. Alla P. Toropova of the Mario Negri Institute for  
560 Pharmacological Research (Italy) for their support in the use of the CORAL software.

561

### 562 **References**

- 563 1. Lövestam, G., Rauscher, H., Roebben, G., Klüttgen, B. S., Gibson, N., Putaud, J.-P., & Stamm, H.  
564 (2010). Considerations on a definition of nanomaterial for regulatory purposes: Publications Office.
- 565 2. Bolt, H., Marchan, R., & Hengstler, J. (2013). Recent developments in nanotoxicology. Archives of  
566 toxicology, 1-2.
- 567 3. Kumar, A., & Dhawan, A. (2013). Genotoxic and carcinogenic potential of engineered nanoparticles:  
568 an update. Archives of toxicology, 87(11), 1883-1900.
- 569 4. Gebel, T., Foth, H., Damm, G., Freyberger, A., Kramer, P.-J., Lilienblum, W., Röhl, C., Schupp, T.,  
570 Weiss, C., Wollin, K.-M., Hengstler, J.G. (2014). Manufactured nanomaterials: categorization and  
571 approaches to hazard assessment. Archives of toxicology, 88(12), 2191-2211.
- 572 5. Huo, L., Chen, R., Shi, X., Bai, R., Wang, P., Chang, Y., & Chen, C. (2015). High-Content Screening  
573 for Assessing Nanomaterial Toxicity. Journal of nanoscience and nanotechnology, 15(2), 1143-1149.

- 574 6. Muthuraman, P., Ramkumar, K., & Kim, D. H. (2014). Analysis of dose-dependent effect of zinc oxide  
575 nanoparticles on the oxidative stress and antioxidant enzyme activity in adipocytes. *Applied biochemistry  
576 and biotechnology*, 174(8), 2851-2863.
- 577 7. Sre, P. R., Reka, M., Poovazhagi, R., Kumar, M. A., & Murugesan, K. (2015). Antibacterial and  
578 cytotoxic effect of biologically synthesized silver nanoparticles using aqueous root extract of *Erythrina  
579 indica lam.* *Spectrochimica Acta Part A: Molecular and Biomolecular Spectroscopy*, 135, 1137-1144.
- 580 8. El Mahdy, M. M., Eldin, T. A. S., Aly, H. S., Mohammed, F. F., & Shaalan, M. I. (2015). Evaluation  
581 of hepatotoxic and genotoxic potential of silver nanoparticles in albino rats. *Experimental and  
582 Toxicologic Pathology*, 67(1), 21-29.
- 583 9. Donaldson, K., & Poland, C. A. (2013). Nanotoxicity: challenging the myth of nano-specific toxicity.  
584 *Current opinion in biotechnology*, 24(4), 724-734.
- 585 10. Lynch, I., Weiss, C., & Valsami-Jones, E. (2014). A strategy for grouping of nanomaterials based on  
586 key physico-chemical descriptors as a basis for safer-by-design NMs. *Nano Today*, 9(3), 266-270.
- 587 11. OECD. (2014). Guidance on grouping of chemicals. Series on testing and assessment No. 194 (second  
588 ed.).
- 589 12. Miller, J. B., & Hobbie, E. K. (2013). Nanoparticles as macromolecules. *Journal of Polymer Science  
590 Part B: Polymer Physics*, 51(16), 1195-1208.
- 591 13. Stefaniak, A. B., Hackley, V. A., Roebben, G., Ehara, K., Hankin, S., Postek, M. T., Lynch, I., Fu,  
592 W.-E., Linsinger, T. P. J., & Thünemann, A. F. (2013). Nanoscale reference materials for environmental,  
593 health and safety measurements: needs, gaps and opportunities. *Nanotoxicology*, 7(8), 1325-1337.
- 594 14. Puzyn, T., Rasulev, B., Gajewicz, A., Hu, X., Dasari, T. P., Michalkova, A., Hwang, H.-M., Toropov,  
595 A. A., Leszczynska, D., & Leszczynski, J. (2011). Using nano-QSAR to predict the cytotoxicity of  
596 metal oxide nanoparticles. *Nature nanotechnology*, 6(3), 175-178.
- 597 15. Ying, J., Zhang, T., & Tang, M. (2015). Metal Oxide Nanomaterial QNAR Models: Available  
598 Structural Descriptors and Understanding of Toxicity Mechanisms. *Nanomaterials*, 5(4), 1620-1637.
- 599 16. Winkler, D. A. (2015). Recent advances, and unresolved issues, in the application of computational  
600 modelling to the prediction of the biological effects of nanomaterials. *Toxicology and applied  
601 pharmacology*.
- 602 17. Gramatica, P., Chirico, N., Papa, E., Cassani, S., & Kovarich, S. (2013). QSARINS: A new software  
603 for the development, analysis, and validation of QSAR MLR models. *Journal of Computational  
604 Chemistry*, 34(24), 2121-2132.
- 605 18. Bigdeli, A., Hormozi-Nezhad, M. R., & Parastar, H. (2015). Using nano-QSAR to determine the most  
606 responsible factor (s) in gold nanoparticle exocytosis. *RSC Advances*, 5(70), 57030-57037.
- 607 19. Müller, K.-R., Mika, S., Rätsch, G., Tsuda, K., & Schölkopf, B. (2001). An introduction to kernel-  
608 based learning algorithms. *Neural Networks, IEEE Transactions on*, 12(2), 181-201.
- 609 20. Hsu, C.-W., Chang, C.-C., & Lin, C.-J. (2003). A practical guide to support vector classification.
- 610 21. Panaye, A., Fan, B., Doucet, J., Yao, X., Zhang, R., Liu, M., & Hu, Z. (2006). Quantitative structure-  
611 toxicity relationships (QSTRs): A comparative study of various non linear methods. General regression  
612 neural network, radial basis function neural network and support vector machine in predicting toxicity of  
613 nitro-and cyano-aromatics to *Tetrahymena pyriformis* §. *SAR and QSAR in Environmental Research*,  
614 17(1), 75-91.
- 615 22. Liu, R., Rallo, R., Weissleder, R., Tassa, C., Shaw, S., & Cohen, Y. (2013). Nano-SAR development  
616 for bioactivity of nanoparticles with considerations of decision boundaries. *Small*, 9(9-10), 1842-1852.
- 617 23. Liu, R., Rallo, R., Bilal, M., & Cohen, Y. (2015). Quantitative structure-activity relationships for  
618 cellular uptake of surface-modified nanoparticles. *Combinatorial chemistry & high throughput screening*,  
619 18(4), 365-375.
- 620 24. Breiman, L. (2001). Random forests. *Machine learning*, 45(1), 5-32.

- 621 25. Svetnik, V., Liaw, A., Tong, C., Culberson, J. C., Sheridan, R. P., & Feuston, B. P. (2003). Random  
622 forest: a classification and regression tool for compound classification and QSAR modeling. *Journal of*  
623 *chemical information and computer sciences*, 43(6), 1947-1958.
- 624 26. Toropov, A. A., Toropova, A. P., Mukhamedzhanova, D. V., & Gutman, I. (2005). Simplified  
625 molecular input line entry system (SMILES) as an alternative for constructing quantitative structure-  
626 property relationships (QSPR). *INDIAN JOURNAL OF CHEMISTRY SECTION A*, 44(8), 1545.
- 627 27. Liaw, A., & Wiener, M. (2002). Classification and regression by randomForest. *R news*, 2(3), 18-22.
- 628 28. Sizochenko, N., Jagiello, K., Leszczynski, J., & Puzyn, T. (2015). How the “Liquid Drop” Approach  
629 Could Be Efficiently Applied for Quantitative Structure–Property Relationship Modeling of Nanofluids.  
630 *The Journal of Physical Chemistry C*, 119(45), 25542-25547.
- 631 29. Goldberg, E., Scheringer, M., Bucheli, T. D., & Hungerbühler, K. (2015). Prediction of nanoparticle  
632 transport behavior from physicochemical properties: machine learning provides insights to guide the next  
633 generation of transport models. *Environmental Science: Nano*, 2(4), 352-360.
- 634 30. Ngamwongsatit, P., Banada, P. P., Panbangred, W., & Bhunia, A. K. (2008). WST-1-based cell  
635 cytotoxicity assay as a substitute for MTT-based assay for rapid detection of toxigenic *Bacillus* species  
636 using CHO cell line. *Journal of Microbiological Methods*, 73(3), 211-215.
- 637 31. Mosmann, T. (1983). Rapid colorimetric assay for cellular growth and survival: application to  
638 proliferation and cytotoxicity assays. *Journal of immunological methods*, 65(1-2), 55-63.
- 639 32. Domey, J., Haslauer, L., Grau, I., Strobel, C., Kettering, M., & Hilger, I. (2013). Probing the  
640 cytotoxicity of nanoparticles: experimental pitfalls and artifacts.
- 641 33. OECD. (2012). Guidance on sample preparation and dosimetry for the safety testing on manufactured  
642 nanomaterials (version of 20 June 2012).
- 643 34. Martin, J. K., & Hirschberg, D. S. (1996). Small sample statistics for classification error rates I: Error  
644 rate measurements: *Information and Computer Science*, University of California, Irvine.
- 645 35. Hawkins, D. M., Basak, S. C., & Mills, D. (2003). Assessing model fit by cross-validation. *Journal of*  
646 *chemical information and computer sciences*, 43(2), 579-586.
- 647 36. Alexander, D., Tropsha, A., & Winkler, D. A. (2015). Beware of R 2: Simple, Unambiguous  
648 Assessment of the Prediction Accuracy of QSAR and QSPR Models. *Journal of chemical information*  
649 *and modeling*, 55(7), 1316-1322.
- 650 37. Hawkins, D. M. (2004). The problem of overfitting. *Journal of chemical information and computer*  
651 *sciences*, 44(1), 1-12.
- 652 38. Low, Y., Uehara, T., Minowa, Y., Yamada, H., Ohno, Y., Urushidani, T., Alexander Sedykh, A.,  
653 Muratov, E., Kuz'min, V., Fourches, D., Zhu, H., Rusyn, I., & Tropsha, A. (2011). Predicting drug-  
654 induced hepatotoxicity using QSAR and toxicogenomics approaches. *Chemical research in toxicology*,  
655 24(8), 1251-1262.
- 656 39. Marchese Robinson, R. L., Glen, R. C., & Mitchell, J. B. O. (2011). Development and comparison of  
657 hERG blocker classifiers: Assessment on different datasets yields markedly different results. *Molecular*  
658 *Informatics*, 30(5), 443-458.
- 659 40. Manganelli, S., Leone, C., manganelli, A. A., Toropova, A. P., & Benfenati, E. (2016). QSAR model  
660 for predicting cell viability of human embryonic kidney cells exposed to SiO<sub>2</sub> nanoparticles.  
661 *Chemosphere*, 144, 995-1001.
- 662 41. Toropov, A. A., Toropova, A. P., Veselinovic, A. M., Veselinovic, J. B., Nesmerak, K., Raska, J.,  
663 Duchowicz, P. A., Castro, E. O., Kudyshkin, V., Leszczynska, D., Leszczynski, J., Leszczynska, D.  
664 (2015). The Monte Carlo Method Based on Eclectic Data as an Efficient Tool for Predictions of Endpoints  
665 for Nanomaterials-Two Examples of Application. *Combinatorial chemistry & high throughput screening*,  
666 18(4), 376-386.

- 667 42. Toropov, A. A., & Toropova, A. P. (2014). Optimal descriptor as a translator of eclectic data into  
668 endpoint prediction: Mutagenicity of fullerene as a mathematical function of conditions. *Chemosphere*,  
669 104, 262-264.
- 670 43. Toropov, A. A., Toropova, A. P., Benfenati, E., Gini, G., Puzyn, T., Leszczynska, D., & Leszczynski,  
671 J. (2012). Novel application of the CORAL software to model cytotoxicity of metal oxide nanoparticles  
672 to bacteria *Escherichia coli*. *Chemosphere*, 89(9), 1098-1102.
- 673 44. Palczewska, A., Palczewski, J., Marchese Robinson, R. L., & Neagu, D. (2014). Interpreting random  
674 forest classification models using a feature contribution method *Integration of Reusable Systems* (pp.  
675 193-218): Springer.
- 676 45. Kuz'min, V. E., Polishchuk, P. G., Artemenko, A. G., & Andronati, S. A. (2011). Interpretation of  
677 QSAR models based on random forest methods. *Molecular Informatics*, 30(6-7), 593-603.
- 678 46. Eriksson, L., Jaworska, J., Worth, A. P., Cronin, M. T., McDowell, R. M., & Gramatica, P. (2003).  
679 Methods for reliability and uncertainty assessment and for applicability evaluations of classification-and  
680 regression-based QSARs. *Environmental health perspectives*, 111(10), 1361.
- 681 47. Oksel, C., Ma, C., & Wang, X. (2015). Current situation on the availability of nanostructure-  
682 biological activity data. *SAR and QSAR in Environmental Research*, 26(2), 79-94.
- 683 48. Ballester, P. J., & Mitchell, J. B. (2010). A machine learning approach to predicting protein-ligand  
684 binding affinity with applications to molecular docking. *Bioinformatics*, 26(9), 1169-1175.
- 685 49. Marchese Robinson, R. L., Lynch, I., Peijnenburg, W., Rumble, J., Klaessig, F., Marquardt, C.,  
686 Rauscher, H., Puzyn, T., Purian, R., Åberg, C., Karcher, S., Vriens, H., Hoet, P., Hoover, M. D., Hendren,  
687 C. O., & Harper, S. L. (2016). How should the completeness and quality of curated nanomaterial data be  
688 evaluated? *Nanoscale*.
- 689 50. Toropova, A. P., Toropov, A. A., Manganelli, S., Leone, C., Baderna, D., Benfenati, E., & Fanelli, R.  
690 (2016). Quasi-SMILES as a tool to utilize eclectic data for predicting the behavior of nanomaterials.  
691 *NanoImpact*.
- 692 51. Kim, I.-Y., Joachim, E., Choi, H., & Kim, K. (2015). Toxicity of silica nanoparticles depends on size,  
693 dose, and cell type. *Nanomedicine: Nanotechnology, Biology and Medicine*, 11(6), 1407-1416.
- 694 52. Rong, Y., Zhou, T., Cheng, W., Guo, J., Cui, X., Liu, Y., & Chen, W. (2013). Particle-size-dependent  
695 cytokine responses and cell damage induced by silica particles and macrophages-derived mediators in  
696 endothelial cell. *Environmental toxicology and pharmacology*, 36(3), 921-928.
- 697 53. Tokgun, O., Demiray, A., Kaya, B., Karagür, E. R., Demir, E., Burunkaya, E., & Akça, H. (2015).  
698 SILICA NANOPARTICLES CAN INDUCE APOPTOSIS VIA DEAD RECEPTOR AND CASPASE 8  
699 PATHWAY ON A549 CELLS.
- 700 54. Donaldson, K., Murphy, F. A., Duffin, R., & Poland, C. A. (2010). Asbestos, carbon nanotubes and  
701 the pleural mesothelium: a review of the hypothesis regarding the role of long fibre retention in the parietal  
702 pleura, inflammation and mesothelioma. *Particle and fibre toxicology*, 7(1), 1.
- 703 55. Yu, T., Malugin, A., & Ghandehari, H. (2011). Impact of silica nanoparticle design on cellular toxicity  
704 and hemolytic activity. *ACS nano*, 5(7), 5717-5728.
- 705 56. Fruijtier-Pölloth, C. (2012). The toxicological mode of action and the safety of synthetic amorphous  
706 silica—A nanostructured material. *Toxicology*, 294(2), 61-79.
- 707 57. Cho, W.-S., Duffin, R., Thielbeer, F., Bradley, M., Megson, I. L., MacNee, W., Poland, C. A., Tran,  
708 L., & Donaldson, K. (2012). Zeta potential and solubility to toxic ions as mechanisms of lung  
709 inflammation caused by metal/metal-oxide nanoparticles. *Toxicological Sciences*.
- 710 58. Karunakaran, G., Suriyaprabha, R., Rajendran, V., & Kannan, N. (2015). Effect of contact angle, zeta  
711 potential and particles size on the in vitro studies of Al<sub>2</sub>O<sub>3</sub> and SiO<sub>2</sub> nanoparticles. *Nanobiotechnology*,  
712 IET, 9(1), 27-34.

713 59. Gajewicz, A., Schaeublin, N., Rasulev, B., Hussain, S., Leszczynska, D., Puzyn, T., & Leszczynski,  
714 J. (2015). Towards understanding mechanisms governing cytotoxicity of metal oxides nanoparticles:  
715 Hints from nano-QSAR studies. *Nanotoxicology*, 9(3), 313-325.

716

717

718

719

720

721

722

723

724

725

726

727

728

729

730

731

732

733

734

735

736

737

738

739

740

741

742

743

744

745

746

747

748

749



750 **Tables**

751 Table 1: In vitro WST-1 cytotoxicity experimental data of silica nanomaterials used for modelling.  
 752 “Treatment time” and “Cell type” columns are related to the in vitro experimental conditions adopted  
 753 during the experimental test for the exposure duration and cell line model, respectively. “Average size”,  
 754 “Aspect ratio” and “Zeta potential” columns are related to measured physico-chemical properties for size,  
 755 aspect ratio and zeta potential of each nanomaterial, respectively. The average size was calculated from  
 756 two primary size dimensions estimated by TEM or other measurements (see the ESI for more details).  
 757 The “pEC25” column is the modelled variable, namely the negative logarithm, to base 10, of the EC25  
 758 value expressed as surface area of nanomaterial per millilitre (i.e. mm<sup>2</sup>/ml). Units are reported in squared  
 759 brackets for numerical properties.

ID	Treatment time [h]	Cell type	Average size [nm]	Aspect ratio [adimensional]	Zeta potential [mV]	pEC <sub>25</sub> [mm <sup>2</sup> /ml]
119	24	THP-1	20.0	1.4	-46.1	-1.299
104	24	16HBE	46.0	1.2	-40.0	-1.272
186	48	THP-1	18.0	1.6	-43.7	-1.165
105	48	16HBE	46.0	1.2	-40.0	-1.135
101	48	16HBE	27.5	1.2	-40.0	-1.105
100	24	16HBE	27.5	1.2	-40.0	-1.026
102	24	A549	27.5	1.2	-40.0	-0.920
103	48	A549	27.5	1.2	-40.0	-0.872
107	48	A549	46.0	1.2	-40.0	-0.844
106	24	A549	46.0	1.2	-40.0	-0.822
121	24	HaCaT	17.0	1.0	-28.1	-0.394
127	24	THP-1	100.0	1.0	-32.0	-0.281
120	24	A549	17.0	1.0	-28.1	-0.223
129	24	HaCaT	60.0	1.0	-30.6	-0.197
128	24	A549	60.0	1.0	-30.6	-0.147
122	24	NRK-52E	17.0	1.0	-28.1	-0.070
130	24	NRK-52E	60.0	1.0	-30.6	0.059
123	24	THP-1	17.0	1.0	-28.1	0.365
131	24	THP-1	60.0	1.0	-30.6	0.483

760  
 761  
 762  
 763  
 764  
 765  
 766  
 767  
 768

769 Table 2: Labelling approach adopted for building the pseudo-SMILES for CORAL modelling. Each label  
 770 is a character which maps a specific value or a range of values. N.B. For brevity, “Correlated descriptors”  
 771 refers to perfectly correlated descriptors, since the binary descriptors corresponding to the different “Cell  
 772 type” labels are partially correlated. Only results without correlated descriptors were presented in the  
 773 main text.

Descriptor	Experimental value	Correlated descriptors	
		Yes	No
Treatment Time [h]	24	A	A
	48	B	No label
	16HBE	C	C
Cell type	A549	D	D
	HaCaT	E	E
	NRK-52E	F	F
	THP-1	G	G
Average size [nm]	≤ 27.5	H	No label
	> 27.5	I	I
Aspect ratio [adimensional]	= 1.0	J	No label
	> 1.0	K	K
Zeta potential [mV]	≥ -32.0	L	L
	< -32.0	M	No label

774

775

776

777

778

779

780

781

782

783

784

785

786

787

788

789

790

791

792

793 Table 3: Descriptors used for CORAL and Random Forest software. Each descriptor was derived based  
 794 on the presence/absence of the relative single character in the original pseudo-SMILES used as input for  
 795 the CORAL software. Only the approach without correlated descriptors is described.

ID	CORAL: Pseudo-SMILES	Random Forest: Explicit representation of descriptors									pEC <sub>25</sub>
		A	C	D	E	F	G	I	K	L	
119	AGK	1	0	0	0	0	1	0	1	0	-1.299
104	ACIK	1	1	0	0	0	0	1	1	0	-1.272
186	GK	0	0	0	0	0	1	0	1	0	-1.165
105	CIK	0	1	0	0	0	0	1	1	0	-1.135
101	CK	0	1	0	0	0	0	0	1	0	-1.105
100	ACK	1	1	0	0	0	0	0	1	0	-1.026
102	ADK	1	0	1	0	0	0	0	1	0	-0.920
103	DK	0	0	1	0	0	0	0	1	0	-0.872
107	DIK	0	0	1	0	0	0	1	1	0	-0.844
106	ADIK	1	0	1	0	0	0	1	1	0	-0.822
121	AEL	1	0	0	1	0	0	0	0	1	-0.394
127	AGIL	1	0	0	0	0	1	1	0	1	-0.281
120	ADL	1	0	1	0	0	0	0	0	1	-0.223
129	AEIL	1	0	0	1	0	0	1	0	1	-0.197
128	ADIL	1	0	1	0	0	0	1	0	1	-0.147
122	AFL	1	0	0	0	1	0	0	0	1	-0.070
130	AFIL	1	0	0	0	1	0	1	0	1	0.059
123	AGL	1	0	0	0	0	1	0	0	1	0.365
131	AGIL	1	0	0	0	0	1	1	0	1	0.483

796

797

798

799

800

801

802

803

804

805 Table 4: Coefficient of determination ( $R^2$ ) and root-mean-square error (RMSE) statistics for the LOO training and  
806 test sets for both CORAL and Random Forest approaches. LOO was performed five times using five different  
807 training set splits, i.e. five different partitions of a given LOO training set to yield an internal “test set” for  
808 hyperparameters’ selection, for CORAL and five different seeds for Random Forest.  $R^2$  and RMSE values were  
809 computed on the predicted values for each training set. Average and standard error of the mean (here reported in  
810 brackets) for training set results were calculated over the 19 models – one for each instance in the dataset – for  
811 each run of the LOO procedure. These statistics were compared with those obtained from the LOO (i.e. test)  
812 predictions. Global results for training sets were calculating by averaging over all the 95 models developed (i.e.  
813 19 models  $\times$  5 LOO runs) whereas, for test sets, global results were obtained by averaging over the five statistics  
814 resulting from LOO. N.B. For both methods, only results without perfectly correlated descriptors are presented.  
815 For Random Forest, only results without bootstrap sampling are presented.

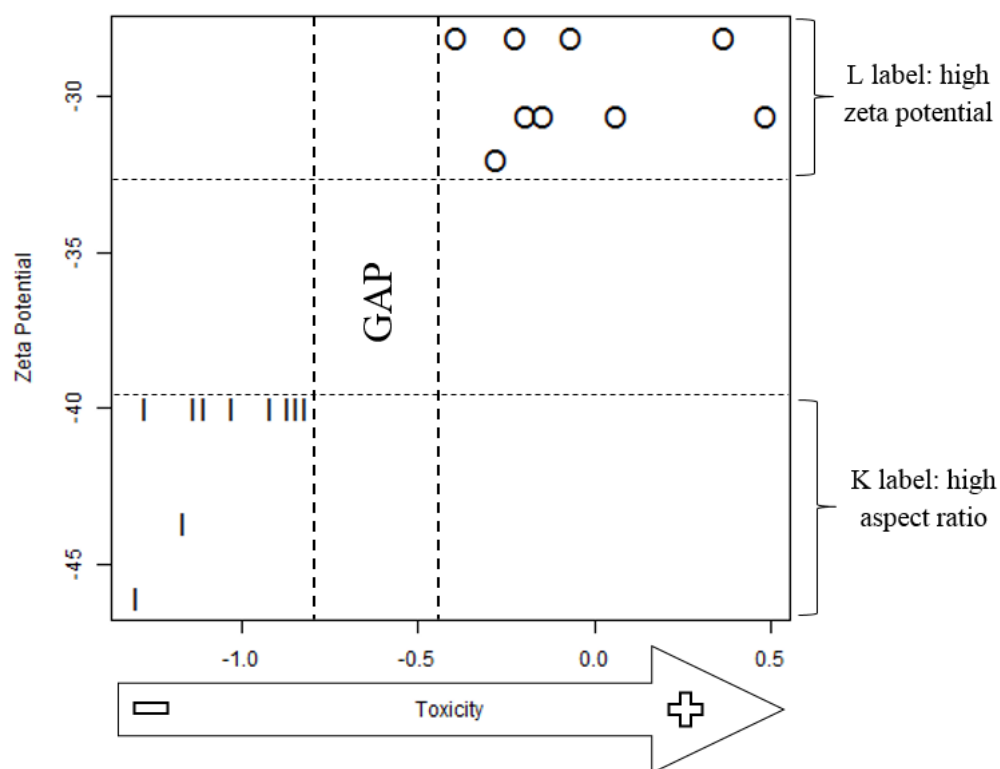
Software	Run	$R^2$		RMSE	
		Training set	Test set	Training set	Test set
CORAL	split 1	0.8031 (0.0166)	0.6529	0.2540 (0.0083)	0.3443
	split 2	0.8567 (0.0056)	0.6243	0.2176 (0.0085)	0.3675
	split 3	0.8570 (0.0029)	0.6143	0.2119 (0.0034)	0.3712
	split 4	0.7876 (0.0077)	0.6436	0.2675 (0.0064)	0.3441
	split 5	0.8383 (0.0108)	0.7082	0.2222 (0.0067)	0.3010
	global	0.8285 (0.0052)	0.6486 (0.0164)	0.2347 (0.0038)	0.3456 (0.0125)
Random Forest	seed 1	0.8717 (0.0023)	0.7741	0.2022 (0.0026)	0.2646
	seed 2	0.8736 (0.0020)	0.7899	0.1995 (0.0023)	0.2544
	seed 3	0.8725 (0.0022)	0.7822	0.2015 (0.0025)	0.2597
	seed 4	0.8711 (0.0023)	0.7707	0.2022 (0.0025)	0.2665
	seed 5	0.8726 (0.0022)	0.7864	0.2004 (0.0025)	0.2568
	global	0.8723 (0.0010)	0.7807 (0.0036)	0.2011 (0.0011)	0.2604 (0.0023)

816

817

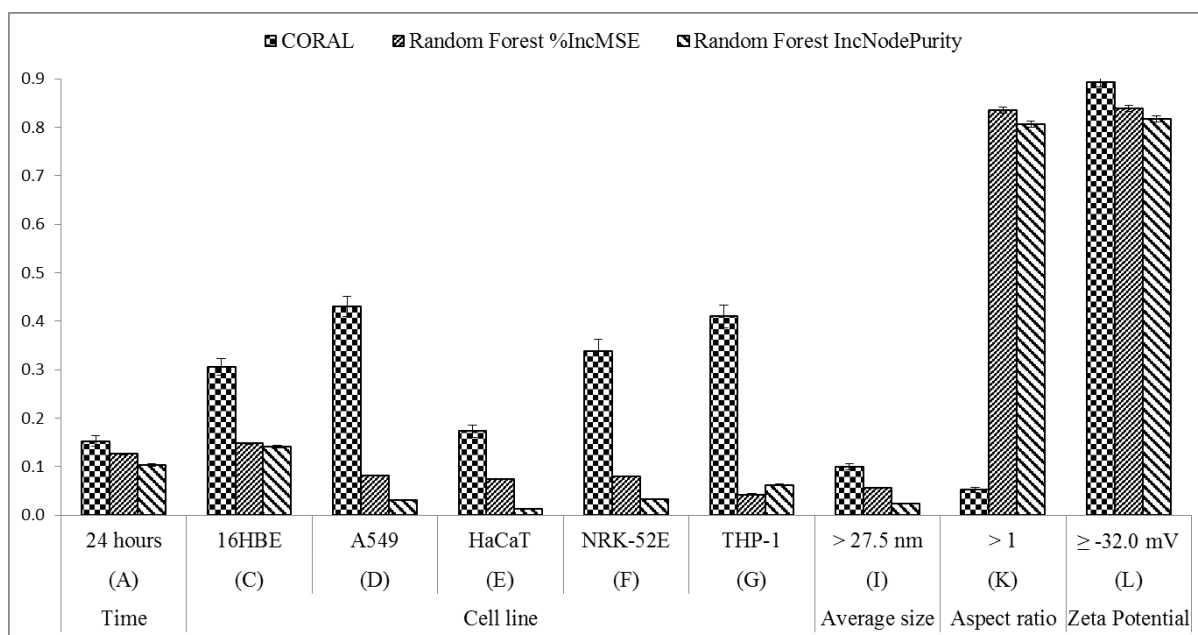
818 **Figures**

819 Figure 1: Zeta potential versus in vitro cytotoxicity experimental values for each silica nanoparticle in the  
820 dataset. The graph shows the gap of toxicological data between -0.822 (ID 106) and -0.394 (ID 121).  
821 With the “I” symbols are indicated silica nanoparticles with aspect ratio greater than 1 whereas the “O”  
822 symbols refer to nanoparticles with aspect ratio equal to 1. N.B. the labels refer to the descriptors used to  
823 encode toxicologically relevant variables for modelling.



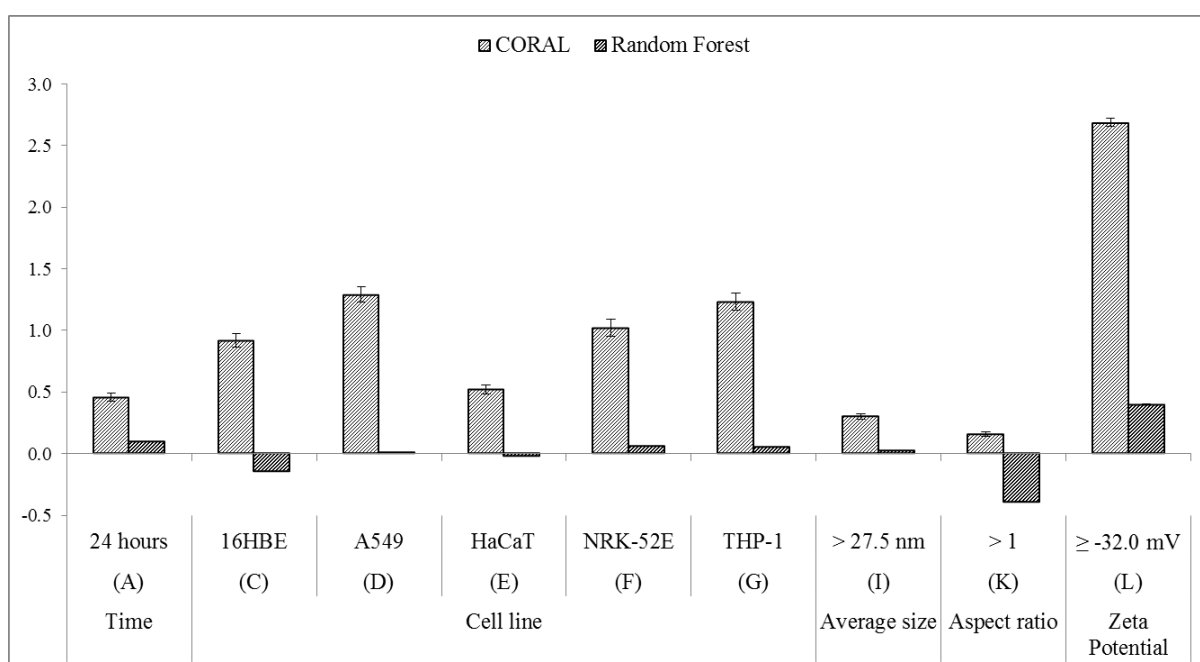
824  
825  
826  
827  
828  
829  
830  
831  
832  
833  
834  
835

836 Figure 2: Average of the scaled variable importance measures for CORAL and Random Forest (without bootstrap  
 837 sampling) methods. N.B. (1) All values were scaled to lie between 1 and 0 by dividing by the range (maximum –  
 838 minimum) of values for each variable importance method. (2) Each binary descriptor takes the value 1 or 0,  
 839 depending upon the value of the corresponding experimental condition or physico-chemical property. Results  
 840 were obtained without perfectly correlated descriptors. Error bars represent the standard error of the mean.



841  
 842  
 843  
 844  
 845  
 846  
 847  
 848  
 849  
 850  
 851  
 852  
 853  
 854  
 855

856 Figure 3: Comparison of the feature contribution results for CORAL and Random Forest methods. For  
 857 CORAL, the “feature contributions” are the correlation weights obtained for a given model built on a  
 858 given LOO training set. For Random Forest, feature contributions were summarised as pseudo-  
 859 coefficients for a given model built on a given LOO training set. The average value was calculated  
 860 across all the 95 models developed on LOO training sets. Error bars represent the standard error of  
 861 the mean. N.B. For both methods, only results without perfectly correlated descriptors are presented.  
 862 For Random Forest, only results without bootstrap sampling are presented.



863  
864  
865  
866  
867  
868  
869  
870  
871  
872

873 **Supplementary Information**

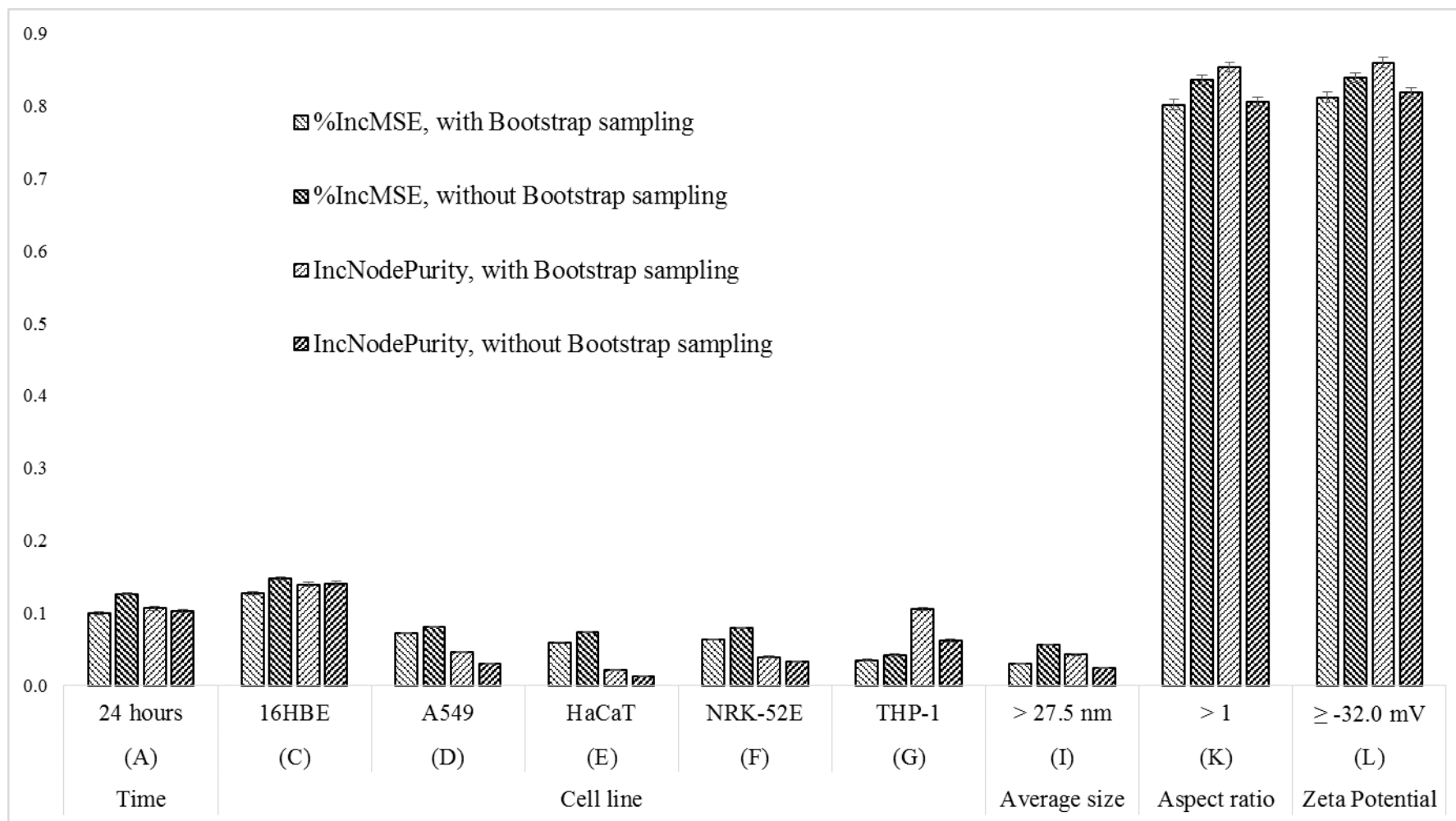
874 Table S1: Summary of the comparison between CORAL and Random Forest approaches. The average and standard error of the mean (in parentheses) of the coefficient of  
 875 determination (R<sup>2</sup>) and the root-mean-square error (RMSE) were calculated across the 95 models developed in leave-one-out on different subsets. For Random Forest, the out-  
 876 of-bag (OOB) subset refers to the results obtained by predicting the training set based on out-of-bag samples and, otherwise, training set predictions were made via applying  
 877 all trees in the model to each training set instance. We considered the influence of correlated descriptors on both methods. N/A = not applicable. As explained in the main text,  
 878 “no” correlated descriptors refers to the absence of perfectly correlated descriptors.

Software	Correlated descriptors	Bootstrap sampling	LOO subset	Run 1		Run 2		Run 3		Run 4		Run 5		Global			
				R <sup>2</sup>	RMSE	R <sup>2</sup>	RMSE	R <sup>2</sup>	RMSE	R <sup>2</sup>	RMSE	R <sup>2</sup>	RMSE	R <sup>2</sup>	RMSE		
CORAL	Yes	N/A	Training		0.8144 (0.0074)	0.2519 (0.0057)	0.8200 (0.0311)	1.0537 (0.8322)	0.8528 (0.0037)	0.2157 (0.0034)	0.7838 (0.0085)	0.2688 (0.0066)	0.8444 (0.0053)	0.2229 (0.0060)	0.8231 (0.0071)	0.4026 (0.1663)	
			Test		0.6053	0.3916	0.0293	7.8504	0.6465	0.3708	0.6508	0.3336	0.6303	0.3661	0.5124 (0.1210)	1.8625 (1.4970)	
	No		Training		0.8031 (0.0166)	0.2540 (0.0083)	0.8567 (0.0056)	0.2176 (0.0085)	0.8570 (0.0029)	0.2119 (0.0034)	0.7876 (0.0077)	0.2675 (0.0064)	0.8383 (0.0108)	0.2222 (0.0067)	0.8285 (0.0052)	0.2347 (0.0038)	
			Test		0.6529	0.3443	0.6243	0.3675	0.6143	0.3712	0.6436	0.3441	0.7082	0.3010	0.6486 (0.0164)	0.3456 (0.0125)	
Random Forest	Yes	Yes	Training	OOB	0.7866 (0.0040)	0.2533 (0.0030)	0.7897 (0.0040)	0.2514 (0.0029)	0.7884 (0.0032)	0.2523 (0.0028)	0.7875 (0.0046)	0.2526 (0.0033)	0.7897 (0.0042)	0.2515 (0.0031)	0.7884 (0.0018)	0.2522 (0.0013)	
				Predicted	0.8985 (0.0025)	0.1758 (0.0026)	0.9000 (0.0024)	0.1743 (0.0026)	0.8985 (0.0022)	0.1755 (0.0024)	0.8991 (0.0026)	0.1751 (0.0028)	0.9000 (0.0026)	0.1744 (0.0027)	0.8992 (0.0011)	0.1750 (0.0012)	
			Test		0.7981	0.2468	0.7996	0.2459	0.7959	0.2481	0.7940	0.2494	0.7901	0.2519	0.7955 (0.0017)	0.2484 (0.0010)	
			No	Training	OOB	0.7869 (0.0032)	0.2530 (0.0028)	0.7911 (0.0032)	0.2504 (0.0026)	0.7932 (0.0035)	0.2491 (0.0027)	0.7894 (0.0032)	0.2515 (0.0027)	0.7919 (0.0030)	0.2500 (0.0027)	0.7905 (0.0014)	0.2508 (0.0012)
					Predicted	0.8732 (0.0018)	0.1961 (0.0022)	0.8743 (0.0021)	0.1953 (0.0022)	0.8742 (0.0021)	0.1953 (0.0023)	0.8752 (0.0021)	0.1944 (0.0022)	0.8743 (0.0020)	0.1953 (0.0023)	0.8742 (0.0009)	0.1953 (0.0010)
				Test		0.7857	0.2542	0.7896	0.2519	0.7927	0.2500	0.7920	0.2505	0.7977	0.2470	0.7915 (0.0020)	0.2507 (0.0012)
	No	Yes	Training	OOB	0.7792 (0.0047)	0.2594 (0.0032)	0.7805 (0.0043)	0.2591 (0.0028)	0.7819 (0.0051)	0.2574 (0.0035)	0.7801 (0.0040)	0.2591 (0.0030)	0.7772 (0.0042)	0.2606 (0.0031)	0.7798 (0.0020)	0.2591 (0.0014)	
				Predicted	0.8989 (0.0026)	0.1795 (0.0027)	0.8989 (0.0024)	0.1793 (0.0025)	0.8993 (0.0026)	0.1782 (0.0027)	0.8990 (0.0024)	0.1789 (0.0025)	0.8985 (0.0025)	0.1792 (0.0026)	0.8989 (0.0011)	0.1790 (0.0011)	
			Test		0.7757	0.2617	0.7896	0.2544	0.7744	0.2622	0.7900	0.2538	0.7867	0.2559	0.7833 (0.0034)	0.2576 (0.0018)	
		No	Training	OOB	0.7732 (0.0049)	0.2644 (0.0038)	0.7854 (0.0030)	0.2563 (0.0026)	0.7737 (0.0030)	0.2641 (0.0028)	0.7723 (0.0042)	0.2642 (0.0034)	0.7717 (0.0039)	0.2639 (0.0031)	0.7753 (0.0018)	0.2626 (0.0014)	
				Predicted	0.8717 (0.0023)	0.2022 (0.0026)	0.8736 (0.0020)	0.1995 (0.0023)	0.8725 (0.0022)	0.2015 (0.0025)	0.8711 (0.0023)	0.2022 (0.0025)	0.8726 (0.0022)	0.2004 (0.0025)	0.8723 (0.0010)	0.2011 (0.0011)	
			Test		0.7741	0.2646	0.7899	0.2544	0.7822	0.2597	0.7707	0.2665	0.7864	0.2568	0.7807 (0.0036)	0.2604 (0.0023)	

879

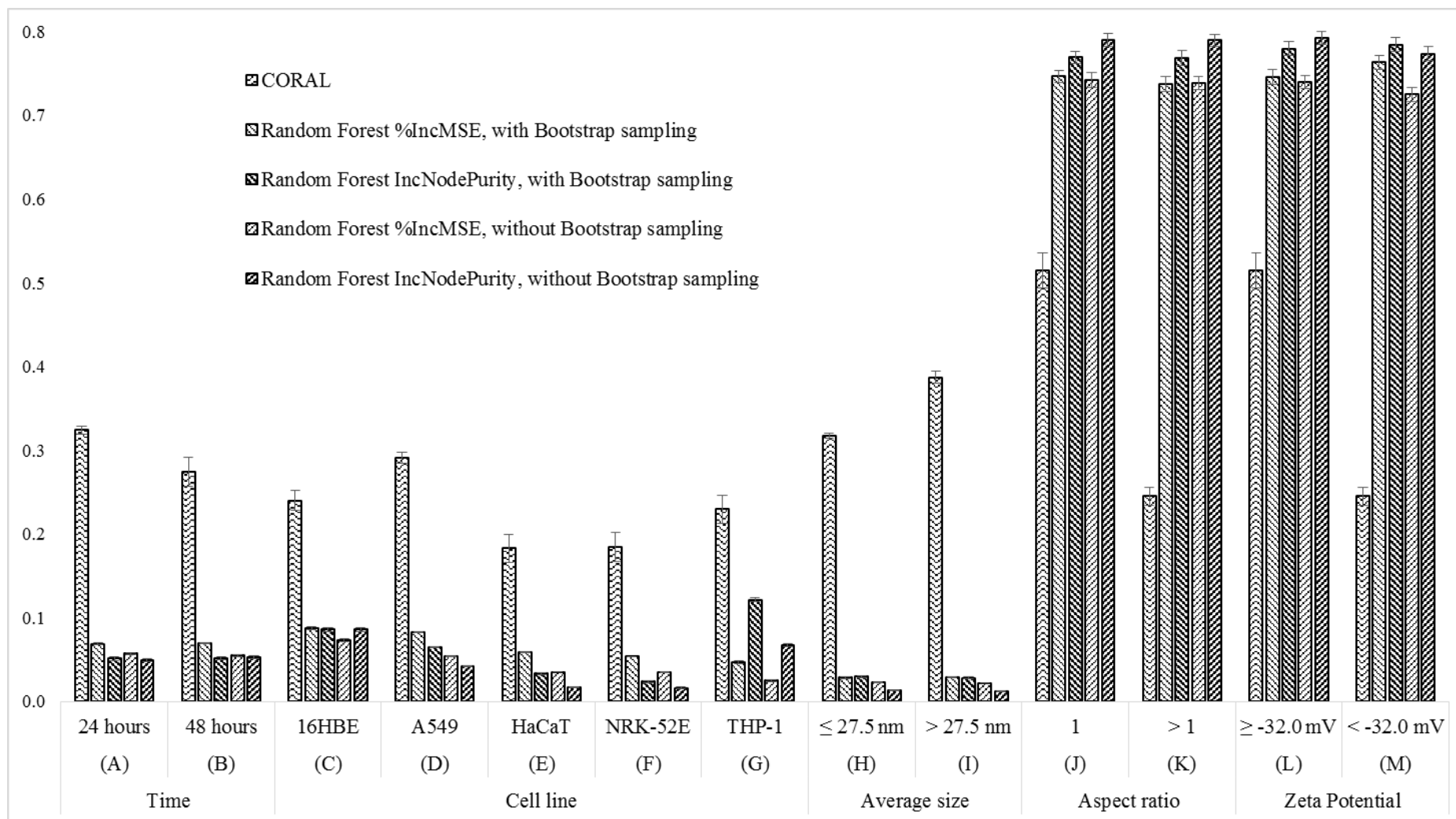


880 Figure S1: Comparison between Random Forest %IncMSE and IncNodePurity scaled variable importance methods with and without bootstrap sampling. Average and standard  
 881 error of the mean (SEM) – here reported as error bar - were calculated across all the models developed by LOO. Perfectly correlated descriptors were deleted.



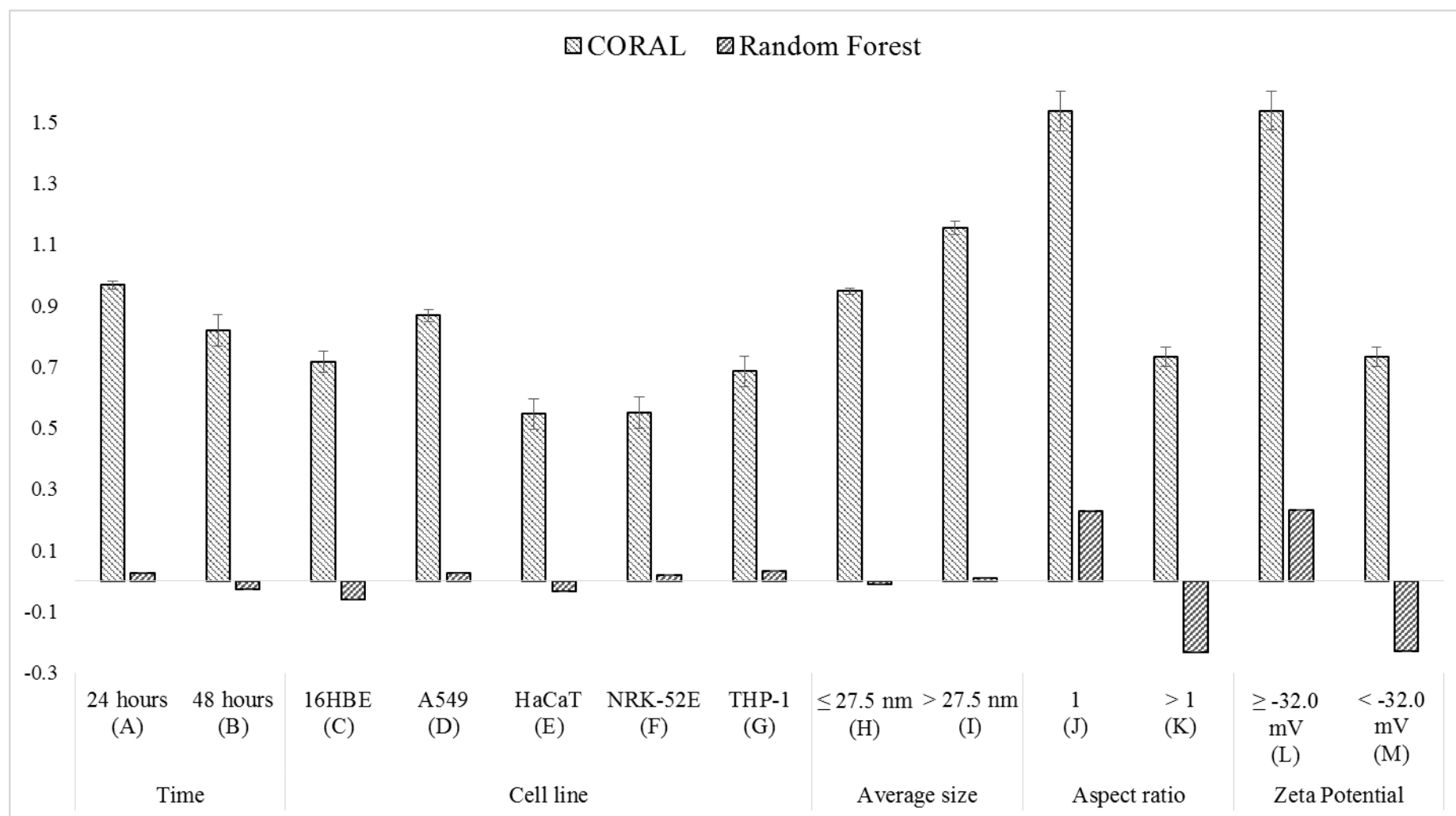
882

883 Figure S2: Comparison between scaled variable importance results for CORAL and Random Forest, including perfectly correlated descriptors. Average and standard error of  
 884 the mean (SEM) – here reported as error bars - were calculated across all the models developed by LOO.



885

886 Figure S3: Feature contribution analysis for CORAL and Random Forest methods with correlated descriptors. Error bars represent the standard error of the mean.



887

888

## 889 **Details on the CORAL software settings and optimisation**

890 As reported in the CORAL software documentation (version: December 17, 2014 for Microsoft Windows,  
891 available at <http://www.insilico.eu/coral/>), in order to use the software, specific text files must be prepared as  
892 input. The CORAL software requires the dataset used for model development to be split into three subsets, each  
893 of which is labelled with a different character in the input file, termed “sub-training” (“+”), “calibration” (“-“) and  
894 “test” (“#”) subsets. (Since the model hyperparameters may be optimised based upon performance on this “test”  
895 set, it may be considered an internal “test” set.) Each of these must contain a minimum number of 3 instances  
896 having a similar experimental range in order for the software to work properly. The exact CORAL settings we  
897 used in this work are shown in Figure S4. In this work we applied the “additive scheme” for which the optimal  
898 descriptor DCW is calculated by summing the correlation weights CWs of each single attribute  $S_k$  which is present  
899 in the input pseudo-SMILES (see main text). Moreover, we selected the “classic scheme” which doesn’t use the  
900 “calibration” subset. The input files we used do contain instances with the “-“ label for calibration subset but this  
901 label was automatically converted by the software into the “+” label for the sub-training subset (see input and  
902 output files in Supplementary Information). We applied the recommended approach [40, 42] of optimising the  
903 CORAL hyperparameters (i.e. the threshold and number of epochs, “T” and “N”) on the internal test set i.e.  
904 instances labelled with “#” (see input files). According to the recommended approach, we prepared five splits of  
905 the same input dataset by shuffling the instances between training and test subsets with the rationale of having a  
906 similar experimental range among the subsets. Table S2 shows the five different splits we used in this work. For  
907 the LOO calculation, a Python script was written to create 19 input text files each containing 18 instances for  
908 CORAL modelling (see Supplementary Information). For each time the CORAL software was used for modelling,  
909 the single item external test set was predicted using the “Start of DCW and Endpoint Calculation for inserted  
910 SMILES” button as shown in Figure S5.

## 911 **Computational resources used to carry out the calculations**

912 We performed all the calculations, including with Random Forest, on a 32-bit Windows 7 machine with an Intel®  
913 Core™ i3-2120 CPU 3.30 GHz processor and 4 GB of installed memory (RAM).

914

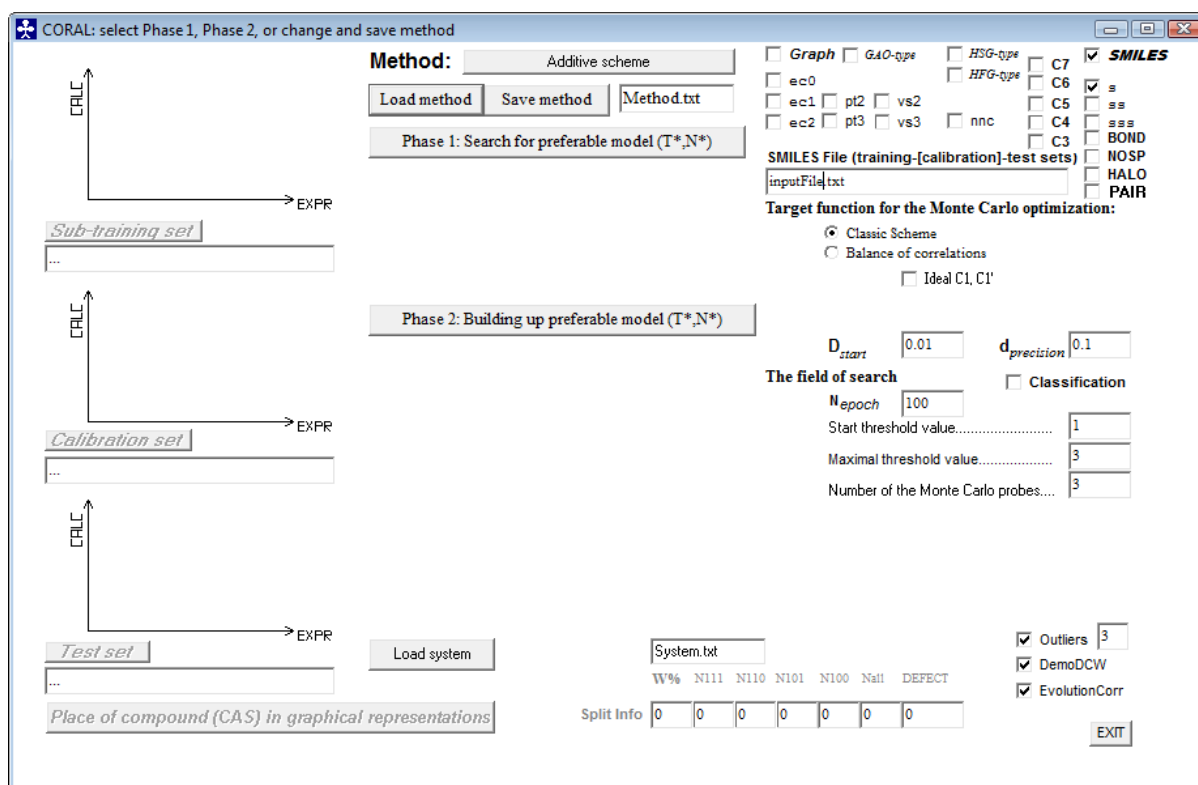
915

916

917

918

919 Figure S4: CORAL graphical user interface settings used in this work.



920  
921  
922  
923  
924  
925  
926  
927  
928  
929  
930  
931  
932  
933  
934  
935  
936  
937  
938

939 Table S2: ID and experimental values (EXP column) for each split of the dataset used for CORAL modelling.  
 940 N.B. (1) The “+”, “-” and “#” symbols stand for sub-training, calibration and test subsets, respectively. (2) For  
 941 “external” LOO validation, one instance was removed at a time and not used for model optimisation, which was  
 942 performed on the internal “test” subset (“#”), i.e. each of these splits of the dataset corresponds to a different split  
 943 of the corresponding LOO training set.

Subset	Split 1		Split 2		Split 3		Split 4		Split 5	
	ID	EXP	ID	EXP	ID	EXP	ID	EXP	ID	EXP
+	119	-1.299	119	-1.299	119	-1.299	119	-1.299	119	-1.299
+	105	-1.135	100	-1.026	105	-1.135	105	-1.135	105	-1.135
+	102	-0.920	102	-0.920	102	-0.920	102	-0.920	107	-0.844
+	106	-0.822	106	-0.822	127	-0.281	106	-0.822	106	-0.822
+	120	-0.223	128	-0.147	120	-0.223	120	-0.223	128	-0.147
+	123	0.365	123	0.365	123	0.365	128	-0.147	100	-1.026
+	131	0.483	131	0.483	131	0.483	131	0.483	131	0.483
-	104	-1.272	104	-1.272	104	-1.272	104	-1.272	104	-1.272
-	101	-1.105	127	-0.281	101	-1.105	101	-1.105	101	-1.105
-	103	-0.872	107	-0.844	100	-1.026	100	-1.026	103	-0.872
-	121	-0.394	121	-0.394	107	-0.844	121	-0.394	121	-0.394
-	129	-0.197	129	-0.197	129	-0.197	129	-0.197	129	-0.197
-	130	0.059	130	0.059	130	0.059	130	0.059	130	0.059
#	186	-1.165	186	-1.165	186	-1.165	186	-1.165	186	-1.165
#	100	-1.026	105	-1.135	103	-0.872	127	-0.281	123	0.365
#	107	-0.844	103	-0.872	121	-0.394	123	0.365	102	-0.920
#	127	-0.281	101	-1.105	106	-0.822	103	-0.872	127	-0.281
#	128	-0.147	120	-0.223	128	-0.147	107	-0.844	120	-0.223
#	122	-0.070	122	-0.070	122	-0.070	122	-0.070	122	-0.070

944

945

946

947

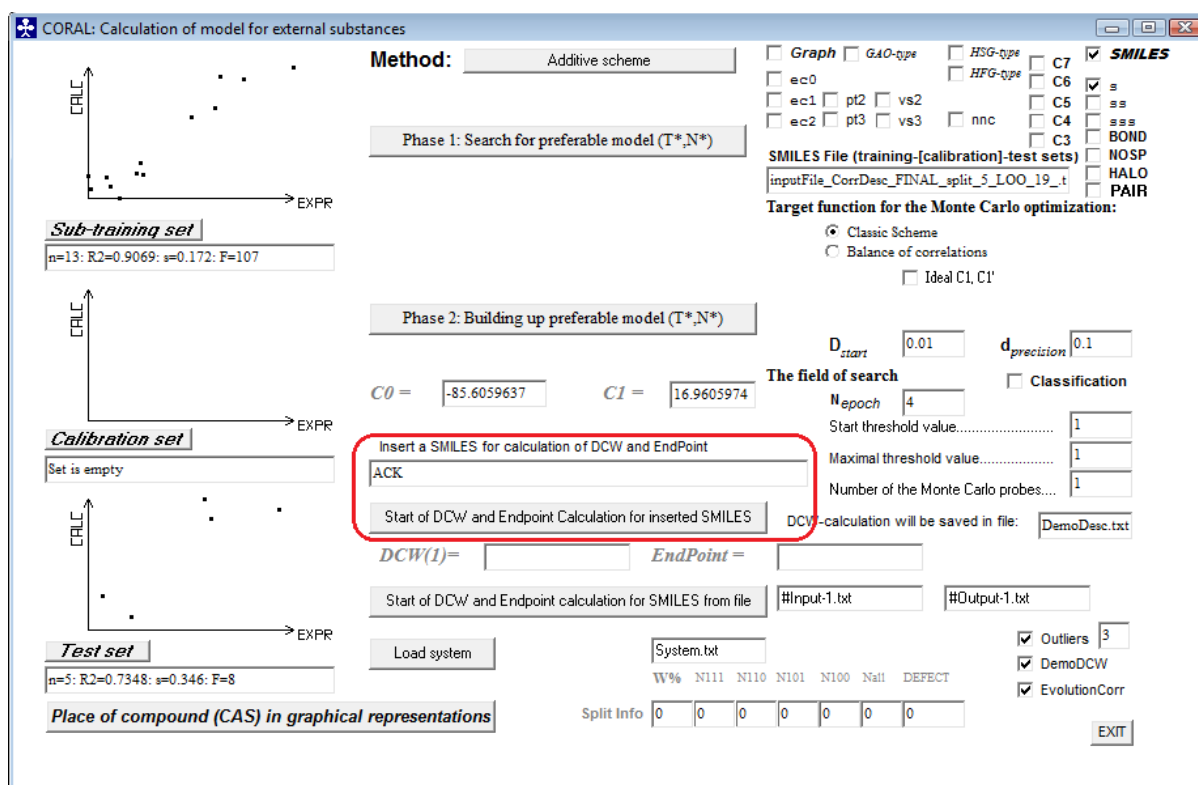
948

949

950

951

952 Figure S5: Screenshot of the CORAL graphical user interface showing an example of calculation of a single item  
 953 external test set for LOO.



954

955

956